scientific reports

Check for updates

OPEN

Proinflammatory cytokines, oxidative stress, and organ function as biomarkers of soman (GD) chronic neurotoxicity

Nyzil Massey[1,4], Suraj S. Vasanthi[1,4], Luis G. Gimenez-Lirola[2], Harm Tyler[3] & Thimmasettappa Thippeswamy[1]✉

Organophosphate (OP) nerve agents, such as soman (GD), pose great risk to neurological health by inhibiting acetylcholinesterase, leading to seizures, epilepsy, and behavioral deficits. While acute treatment may alleviate immediate symptoms, the long-term consequences, particularly those involving neuroinflammation and systemic toxicity, remain poorly understood. This study used adult male and female Sprague Dawley rats to investigate the chronic effects of a single acute exposure to soman (132 µg/kg, s.c., $1.2 \times LD_{50}$) on neuroinflammation, behavioral comorbidity, and systemic toxicity. Following exposure, animals were treated with atropine sulfate (2 mg/kg, i.m.) and oxime HI-6 (125 mg/kg, i.m.) to mitigate peripheral cholinergic effects, and with midazolam (3 mg/kg, i.m., 1 h post-exposure) to control seizures. Spontaneously recurring seizures were monitored during handling and with video electroencephalogram (vEEG). Neurobehavioral deficits were assessed 4–8 weeks post-exposure. At 18 weeks post-exposure, brain, serum, and cerebrospinal fluid (CSF) were analyzed for inflammatory and nitro-oxidative stress markers, and the liver and kidney function biomarkers were evaluated. Soman-exposed animals developed epilepsy, confirmed by handling-induced seizures and/or continuous vEEG monitoring. Behavioral assessments revealed significant memory deficits following soman exposure. Proinflammatory cytokines (TNF-α, IL-6, IL-1α, IL-18, IL-17A, and MCP-1) were significantly elevated in both serum and CSF, alongside corresponding increases in their gene expression in the brain. Elevated reactive oxygen/nitrogen species were detected in the serum. Although hematological parameters remained unchanged, a significant increase in total bilirubin and an upward trend in serum blood urea nitrogen (BUN) levels and BUN: Creatinine ratio indicated potential liver and kidney dysfunction. However, no significant structural changes in these organs at the cellular level were observed in histological analyses. This study identifies critical chronic biomarkers of soman exposure affecting the brain, serum, CSF, liver, and kidney. The findings highlight the critical need to monitor systemic and neurological impacts, as well as organ function, to develop effective diagnostic and therapeutic strategies for survivors of nerve agent exposure or OP pesticide poisoning. Behavioral deficits and EEG changes in soman-exposed animals further emphasize the long-term neurological consequences of exposure.

Keywords Organophosphate nerve agents, Soman, Neuroinflammation, Chronic neurotoxicity, Peripheral biomarkers, Organ function

Organophosphate nerve agents (OPNA) are a class of highly toxic chemical compounds that disrupt the nervous system's ability to transmit neurochemical signals. Due to the potent and volatile nature of the OPNAs, exposure can occur through inhalation, ingestion, or skin contact, with symptoms manifesting rapidly. Soman, also known as GD, is one such OPNA that was initially developed as an insecticide but is now classified as a chemical warfare agent[1]. It inhibits the acetylcholinesterase (AChE), an enzyme critical for nerve and muscle function, leading to the accumulation of acetylcholine (ACh) and overstimulation of neurons and muscles

[1]Department of Biomedical Sciences, College of Veterinary Medicine, Iowa State University, Ames, IA, USA. [2]Vet Diagnostic and Production Animal Medicine, College of Veterinary Medicine, Iowa State University, Ames, IA, USA. [3]Department of Veterinary Pathology, College of Veterinary Medicine, Iowa State University, Ames, IA, USA. [4]Nyzil Massey and Suraj S. Vasanthi contributed equally to this work. ✉email: tswamy@iastate.edu

to initiate a range of neurological effects, including muscle twitching, seizures, and paralysis that can lead to respiratory failure and death[2–4]. The management of cholinergic symptoms and seizures resulting from acute exposure to OPNA is complex and requires atropine, an oxime, and higher doses of antiseizure agents such as benzodiazepines[5]. Despite controlling the symptoms, long-term brain damage follows OPNA exposure[2,3] and may result in cognitive dysfunction[6]. Currently, there are no systemic biomarkers to monitor OPNA-induced chronic systemic toxicity and disease progression.

Neuroinflammation, triggered by OPNA exposure, develops due to the activation of glial cells and the release of pro-inflammatory cytokines, which may exacerbate neuronal hyperexcitability and accelerate the development of epilepsy[7,8]. Particularly, TNF-α and IL-6 have been shown in preclinical and clinical studies to correlate with neurodegeneration and cognitive impairment[9,10]. Reliable peripheral biomarkers from blood and cerebrospinal fluid (CSF) can be helpful in the early detection of neuroinflammation in nerve agent exposure[3]. Studies involving humans and animal models have identified increased levels of pro-inflammatory cytokines in patients with epilepsy, correlating with the frequency of epileptic seizures[11]. Additionally, reactive oxygen/nitrogen species generation has been linked to neuroinflammation following seizures[12]. These biomarkers aid in the diagnosis and may offer potential therapeutic targets to improve the management of nerve agent exposed survivors and provide insights into the pathophysiology of soman-induced epilepsy. Therefore, the identification of such markers is a step forward in the quest for precision medicine in the treatment of epilepsy and its associated complications in OPNA survivors.

OPNAs have been previously shown to be implicated in visceral organ toxicity and alter the complete blood count (CBC)[13]. The liver can be affected due to its role in detoxifying chemicals and metabolizing drugs. The kidneys are also vulnerable as they filter blood and can accumulate toxic substances. Monitoring the liver and kidney function biomarkers can be a diagnostic tool to prevent further injury to these vital organs. Alanine aminotransferase (ALT) and aspartate aminotransferase (AST) are the liver enzymes that metabolize amino acids[14]. Elevated levels of ALT and AST in the blood may indicate liver dysfunction. Total bilirubin, a byproduct of the breakdown of heme in the red blood cells, is an essential biomarker of liver function. Creatinine, a waste product generated from muscle metabolism, is filtered out by the kidneys. Abnormal levels of creatinine in the blood suggest impaired kidney function. BUN is another indicator of kidney function. Elevated BUN levels can be a sign of kidney stress or damage. Together, these markers provide valuable insights into the health and functioning of the liver and kidneys[15].

Our previous studies investigated the impact of acute exposure to diisopropylfluorophosphate (DFP, a 6-week study) and soman exposure (18 weeks study) on various parameters[3,16]. The current study is focused on the interactions between biochemical markers, neuroinflammation, and behavioral outcomes, offering a more comprehensive understanding of chronic soman toxicity by integrating systemic and more central changes in the brain over a prolonged period after acute exposure. There is limited research on how acute soman exposure affects biochemical and blood-related parameters in the context of changes in the brain. The research conducted in 1990 and 2001 reported the short-term effects of low to moderate doses of soman (30 and 90 µg/kg) on blood parameters in mice and rabbits[17–19]. Furthermore, assessments of liver and kidney functions were not reported to determine the potential toxicological impact of soman. To date, there has been no comprehensive data from chronic studies on blood biochemistry, complete blood count, and histopathological changes following acute exposure to a high dose of soman (132 µg/kg, single exposure) that results in *status epilepticus* for > 40 min.

The rationale for studying soman exposure is that it is highly volatile compared to other OPNA agents, such as DFP, and could be abused as a potential chemical warfare agent to target civilians and military personnel. While DFP is considered a surrogate for soman, no published literature demonstrates that the long-term effects observed with DFP (e.g., at 6 weeks post-exposure)[16] could mimic the consequences of soman exposure. We hypothesized that the effects of soman could be long-lasting, and to test this, we used a soman model. Specifically, we selected a dose of soman (1.2 × LD50) to induce severe *status epilepticus* (SE), which triggers the development of spontaneously recurring seizures (SRS). This study, therefore, focuses on the chronic biomarkers observed post-acetylcholinesterase (AChE) inhibition during the SRS phase of disease progression after an acute exposure to soman.

While OPNAs and organophosphate pesticides inhibit AChE, they differ significantly in chemical structure, potency, and intended use[20,21]. OPNAs, such as soman, are synthesized for chemical warfare, rapid onset of action, and highly toxic than OP pesticides[22] used for agricultural applications. These differences necessitate distinct considerations when evaluating their long-term effects. In this study, adult rats were exposed to either vehicle (cold PBS) or soman and euthanized at 18 weeks post-exposure. Initially, soman-exposed rats were monitored for handling-induced seizures in the acute phase of the study (2–15 days post-exposure) and then continuously through vEEG at later time points (10–18 weeks post-soman). Neurobehavioral changes were also assessed at 4–8 weeks post-soman. Finally, all animals were euthanized at 18 weeks post-soman, and various tissues were collected for analysis; brain tissue for cytokines gene expression, CSF and serum for secreted cytokines and nitro-oxidative markers, and whole blood for complete blood count and biochemical analysis. ALT, AST, total bilirubin, creatinine, and BUN levels in serum were evaluated for liver and kidney function. Liver and kidney tissues fixed in 4% paraformaldehyde were evaluated for microscopic pathological changes.

Methods
Animal source, care, ethics statement, and euthanasia
Adult male and female Sprague–Dawley rats (7–8 weeks old, 250–300 g; Charles River, USA) were utilized in this study. In an enriched environment, males and females were housed in the same room in individual cages under a 12-h light/dark cycle. Following 2–3 days of acclimatization, all experiments were conducted in accordance with an approved protocol by the Institutional Animal Care and Use Committee at Iowa State University (IACUC protocol: 23-114) and adhered to the NIH ARRIVE Guidelines for the Care and Use of Laboratory Animals.
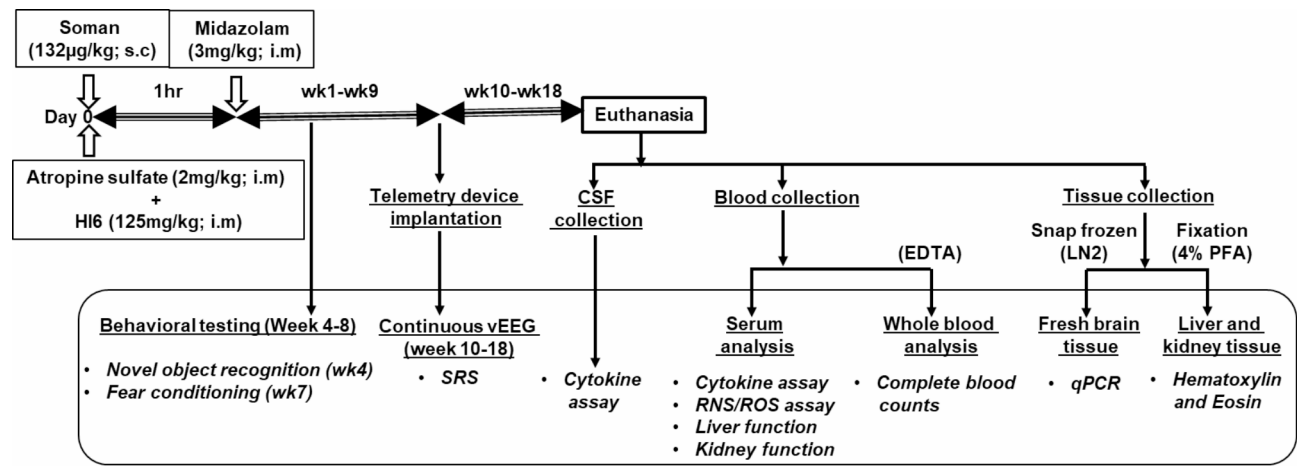
Fig. 1. Experimental design. 18-week study with various treatments, analyses in live animals, and sample collection after euthanasia is shown. *EDTA* ethylenediaminetetraacetic acid, *LN2* liquid nitrogen, *PFA* paraformaldehyde, *vEEG* video EEG, *SRS* spontaneous recurrent seizures.

Groups	Control (n = 24)		Soman (n = 26)	
Tissue type	Fresh	Perfused	Fresh	Perfused
Rats/sex	12 rats (6/sex)	12 rats (6/sex)	13 rats (6–7/sex)	13 rats (6–7/sex)
Randomly chosen for the study*	10 rats (5/sex)	10 rats (5/sex)	10 rats (5/sex)	10 rats (5/sex)*
Used for telemetry	No	No**	No	Yes

Table 1. Number of animals used in experimental groups. *Based on matched SE severity in soman-exposed animals. **Control animals do not seize. Therefore not implanted with a telemetry device.

Soman exposure procedures were performed at MRI Global, Kansas City, MO, while all other experiments were carried out in the Laboratory Animal Resources facility at Iowa State University. After the study (18 weeks), all animals were euthanized using pentobarbital sodium and phenytoin sodium (100 mg/kg, i.p.) in compliance with the American Veterinary Medical Association's Guidelines for Euthanasia.

Chemicals and reagents

The soman (purity > 95% confirmed by GC–MS) was obtained and administered to animals at MRI Global, Kansas City, MO, USA, per approved IACUC protocol. Soman was diluted in cold PBS. HI-6 (99.9% purity, validated by LC/MS; Kalexsyn, Kalamazoo, MI, USA) and atropine sulfate monohydrate (ATS, 99.9% purity, verified by LC–MS; Tokyo Chemical Industry, USA) were diluted in saline to the final concentrations of 250 mg/mL and 5 mg/mL, respectively. All chemicals used in animals were authenticated by LC/GC–MS/MS to confirm purity and identity. Midazolam (MDZ, prepared as a 5 mg/mL stock solution) was supplied by MRI Global. The euthanasia solution, containing pentobarbital sodium and phenytoin sodium, was procured from the Pharmacy at the ISU Lloyd Veterinary Medical Center. The specific details of the assay kits used in this study are provided in the corresponding sections.

Soman exposure, medical countermeasures, and animal numbers

Experimental Design is illustrated in Fig. 1. For this study, we randomly assigned 40 rats (20/sex) from a large cohort of 50 rats. The details about the number of animals used in different analyses are given in Tables 1 and 2. Rats were either treated with vehicle (Cold PBS) or soman (GD, 132 µg/kg, s.c. $1.2 \times LD_{50}$) followed by HI-6 (125 mg/kg, i.m.) and atropine sulfate (2 mg/kg, i.m.) within 1 min of soman exposure to minimize peripheral cholinergic effects and mortality. Anticonvulsant midazolam (3 mg/kg, i.m.) was administered 1 h post-soman exposure to control behavioral SE and mortality due to the severity of SE.

Behavioral seizures and *status epilepticus* (SE) severity analysis

Behavioral seizures were monitored for 60 min post-exposure until the administration of midazolam. Two experimenters per animal scored the seizures in real-time during SE on a scale of 1–5. The stages of seizures (stages 1–5) observed in the soman model, their stage-specific symptoms, and the methods for SE severity quantification are detailed in our publications[2,3]. Briefly: Stage 1: Excessive salivation, lacrimation, urination, defecation (SLUD), mastication, and chewing. Stage 2: Progression of stage 1 symptoms, including tremors, wet-dog shakes, head nodding/neck jerks, kyphosis, and opisthotonos. Stage 3: Forelimb clonus, Straub tail, rearing, and rigid extension of the forelimbs. Stage 4: Repeated rearing, continuous forelimb clonus, and loss of

Analysis	Sample type	Non-perfused rats "n" (m/f)	Perfused rats "n" (m/f)
Cytokines gene expression	Brain tissue (cortex)	10 per group (5/sex)	x
Secreted cytokines	Serum	x	10 per group (5/sex)
	CSF	x	8 per group (4/sex)
Secreted free radicals	Serum	x	10 per group (5/sex)
Hematological parameters	Whole blood	x	10 per group (5/sex)
Liver function test	Serum	x	10 per group (5/sex)
Kidney function test	Serum	x	10 per group (5/sex)
Histology (H&E)	Liver and kidney tissue	x x	10 per group (5/sex) 10 per group (5/sex)
EEG analysis	Live animal	x	**10 (5/sex)
Neurobehavioral tests*	Live animal	10 per group (5/sex)	10 per group (5/sex)

Table 2. Summary of analysis types, sample sources, and group allocation (perfused vs. non-perfused animals). *The behavioral tests were conducted as mixed-sex cohorts (control, 24; soman, 26), but we used the behavioral data from 40 animals (Perfused and non-perfused). **Only soman group.

the righting reflex. Stage 5: Abducted limb clonus and generalized seizures. Animals of both sexes were further categorized based on comparable SE severity and coded for subsequent analysis.

Evaluation of handling-induced seizures
Convulsive seizures were observed in rats twice daily, once in the morning and the evening, during routine husbandry, dosing, or cage cleaning by animal care personnel. Seizures within the first 24 h post-exposure were excluded from the analysis to avoid confounding effects of residual soman in circulation and recovery of AChE activity[23,24]. Handling seizure activity was documented from day 2–15 post-exposure (14 days).

Telemetry device implantation and vEEG-based seizure quantification
To determine whether SE induced by acute soman exposure progressed to epilepsy, 10 rats (5 males and 5 females) were randomly selected and implanted with CTA-F40 telemetry devices (Data Science International, MN, USA) 10 weeks post-exposure. Continuous video-EEG monitoring was then conducted as previously described[16,25,26]. Before surgery, the animals received an analgesic, buprenorphine (0.3 mg/kg, s.c.), and a broad-range antibiotic, enrofloxacin (5 mg/kg, s.c.). For anesthesia, rats were induced with 3.0% isoflurane (at 1 L/min O_2) and maintained at 1.0–1.5% isoflurane during the procedure. The anesthesia was delivered using a SomnoFlo small animal anesthetic machine (Kent Scientific, Torrington, CT, USA). An ointment containing artificial tears was applied to protect the cornea during the surgery. A midline incision was made on the scalp, and the underlying tissue was resected to expose the parietal bone. Bilateral electrodes were implanted on the dura mater of the cortical hemispheres by drilling small holes in the skull. The telemetry device was positioned in a subcutaneous pouch in the flank region. Electrodes were secured to the skull with dental cement (A-M Systems, Carlsborg, WA, USA), and the incision was closed with sterile clips. A triple antibiotic ointment (Vetropolycin) was applied to the wound, and 1 mL of 5% dextrose subcutaneously. Following recovery, the animals were housed individually in cages placed on the PhysioTel receiver pads (RPC-1) connected to the Data Exchange Matrix 2.0 (DSI) for continuous video-EEG acquisition using Ponemah Software (DSI).

Spontaneously recurring seizures (SRS) quantification
Seizure-free and epileptiform-free segment of the EEG trace was identified for each animal to set the baseline parameters to detect SRS and epileptiform spikes. SRS on EEG was identified based on high-frequency and/or high-amplitude epileptiform spikes and matched with simultaneous video input. Artifacts resulting from electrical noise, grooming, and exploratory behavior were identified and excluded from the analysis, as described in detail in our previous publications[25,27]. Seizure detection and analyses were executed using NeuroScore software (version 3.4.0, DSI). All convulsive SRS events identified by the software were manually validated through integrated video recordings for behavioral seizure analysis and by examining the corresponding power spectral changes.

Novel object recognition (NOR) and open-field tests
The NOR test assesses learning and memory in rodents, while the open field test, conducted using the same apparatus, evaluates anxiety-like behavior. Both tests were carried out over three consecutive days: the habituation/open field test day, the testing day, and the probing day. A low-wattage red light illuminated the testing arena (40 × 40 inches)[28]. On the habituation/open field test day, animals could explore the arena for 10 min without any objects. The time spent in the center versus the periphery of the arena was recorded to evaluate open-field behavior. On the testing day, two identical objects (Stoelting Co., USA) were placed diagonally in the arena. The rat was released from a corner opposite the objects and allowed to explore for 5 min. On the probing day (24 h after the testing day), one of the two objects was replaced with a novel object. The rat was again allowed to explore the objects for 5 min. Rats that spent less than 20 s exploring the objects were excluded from the analysis[29]. The movement of the rats was tracked using a camera connected to ANY-Maze software (Stoelting Co., USA). During the habituation phase, time spent in the center versus the periphery was analyzed, while the

discrimination index (DI) was calculated during the probing phase to compare the exploration of the novel object relative to the familiar object: DI = (t_novel − t_familiar)/(t_novel + t_familiar). Results were compared across experimental groups and between sexes.

Contextual and cued fear conditioning test

The contextual and cued fear conditioning test evaluated the rat's ability to recall the association between a conditioned stimulus (an auditory tone) and an aversive unconditioned stimulus (a foot shock). The test consisted of two phases: conditioning (Day 1) and probing (Day 2). On the conditioning day, rats were allowed to explore the apparatus for 2 min before presenting an auditory tone (70–80 dB) lasting 20 s. During the final 2 s of the tone, a continuous 0.7-mA foot shock was delivered. This conditioning sequence was repeated four times within a session, with an 80-s inter-trial interval followed by a rest period of 80 s. The probing session was conducted 24 h later. The protocol was identical to the conditioning session, except no foot shock was delivered. Rat's movements were recorded using a camera connected to ANY-maze software (Stoelting Co., USA). Freezing time during both the conditioning and probing sessions was measured and analyzed. Comparisons were made between experimental groups and sexes. The percent increase in freezing time from the conditioning to the probing session was calculated across all four tones and averaged. The data was presented as mean ± SEM and plotted for further analysis.

Blood, CSF, and other tissues collection

The blood was collected by cardiac puncture under terminal anesthesia. The rat was positioned in a supine position, and the thoracic cavity was opened. Blood was aspirated with a sterile syringe by inserting a 21–25 gauge needle into the left ventricle of the heart through the chest wall. The blood was centrifuged at 1000–1500×*g* for 10 min to separate serum. Aliquots of 300 μL blood were collected in tubes containing ethylenediamine tetra-acetic acid (EDTA-K2) and mixed by inversion for a complete blood count (CBC). The CSF was collected from the cisterna magna under terminal anesthesia. The head was positioned downward at an approximately 45° angle to access CSF at the cisterna magna. A depression between the occipital protuberance and the wing of the atlas was located, and a sterile needle connected to a syringe was inserted perpendicularly into the cisterna magna without an incision to avoid contamination of CSF with blood. Resistance change while inserting the needle into the fourth ventricle of the brain at the cisterna magna indicates the tip of the needle at the target site. Colorless CSF was gently aspirated into the syringe. Both serum and CSF were aliquoted and stored at − 80 °C until further analysis[30]. The fresh brain tissue collected for gene expression analysis was snap-frozen in liquid nitrogen (LN2) and stored at − 80 °C. Liver and kidneys from animals perfused with 4% paraformaldehyde (PFA) were collected and processed for Hematoxylin and Eosin staining for histological evaluation.

Hematological parameters

CBC was performed in an automated ProCyte Dx Hematology Analyzer to measure the following parameters: red blood cell (RBC) count, hematocrit (HCT), hemoglobin, mean corpuscular volume (MCV), mean corpuscular hemoglobin (MCH), mean corpuscular hemoglobin concentration (MCHC), red cell distribution width (RDW), reticulocytes, total white blood cells (WBC), neutrophils, lymphocytes, monocytes, eosinophils and basophiles. The minimum volume of 300 μL blood was used for CBC analysis. Refer to Supplementary Table S1 for mean ± SEM values for all treatment groups.

Blood biochemical analysis

The serum samples were analyzed for alanine transaminase (ALT), aspartate transaminase (AST), Total bilirubin, blood urea nitrogen (BUN), and creatinine using IDEXX Catalyst Chemistry Analyzers. 10 μL of serum was used per analyte. The serum sample, slides, and pipette tips were loaded into the sample drawer and run on the IDEXX VetLab Station. Refer to Supplementary Table S2 for mean ± SEM values for all treatment groups.

RNA isolation and qPCR

The total RNA was extracted from the brain tissue (cortex) using TRIzol reagent (Invitrogen, catalog # 15596-026) according to the instructions by the company. The RNA's purity was assessed with a NanoDrop spectrophotometer, considering an A260/A280 ratio of 1.8–2.1, a suitable quality for subsequent analysis. 1 μg of the RNA was reverse transcribed (RT) to cDNA using the Superscript IV VILO Kit (Thermo Fisher Scientific, catalog#11766050) as per the protocol. The qPCR mix comprised of 5 μL of PowerUp SYBR Green Master mix (Thermo Fisher Scientific, catalog # 25742), 0.5 μL of forward and reverse primers (10 μM concentration), 3 μL of nuclease-free water, and 1 μL of the synthesized cDNA (1–10 ng) was used. Quantstudio™ 3 (Applied Biosystems) was used to run the real-time PCR reactions. Primer sequences from Integrated DNA Technologies were used for the qPCR (Table 3). β-actin served as the reference gene for all gene products. The cycle threshold (CT) values for the target gene products were normalized against the CT values of the reference gene. Group comparisons were conducted using the ΔCT approach, where the ΔCT for each sample was the difference between the CT of the target gene and β-actin. The average ΔCT of the control group was established as the calibrator, which was then deducted from the ΔCT of each sample within the control and experimental groups to calculate the ΔΔCT. Fold changes in gene expression were determined using the formula $2^{-\Delta\Delta Ct}$, and the mean fold change was computed for each experimental group and compared between control and soman-exposed samples.

Luminex assays for cytokine detection in serum and CSF

Customized MILLIPLEX® Rat Cytokine/Chemokine kit (Millipore Sigma, RECYTMAG-65K-08C) was used to assess the levels of TNF-α, IL-6, IL-1α, IL-18, IL-17A, and MCP-1. 25 μL of the sample (serum or CSF) was

Sr. no.	Primer name	Sequence	Sequence 5′–3′
1.	MCP1	Forward	TGTTCACAGTTGCTGCCTG
2.	MCP1	Reverse	GCCGACTCATTGGGATCATC
3.	TNFα	Forward	CAGACCCTCACACTCAGATCATCTTCT
4.	TNFα	Reverse	CCACTTGGTGGTTTGCTACGAC
5.	IL17A	Forward	AGTGAAGGCAGCGGTACT
6.	IL17A	Reverse	CTCAGAGTCCAGGGTGAAGTG
7.	IL-6	Forward	TAGTCCTTCCTACCCCAATTTCCAA
8.	IL-6	Reverse	TTGGTCCTTAGCCACTCCTTC
9.	IL18A	Forward	ACCACTTTGGCAGACTTCAC
10.	IL18A	Reverse	CTGGTCTGGGATTCGTTGG
11.	IL-1α	Forward	GGTAGTGAGACCGACCTCAT
12.	IL-1α	Reverse	GGTGCACCTGACTTTGTTCT
13.	β-actin	Forward	AAGTCCCTCACCCTCCCAAAAG
14.	β-actin	Reverse	AAGCAATGCTGTCACCTTCCC

Table 3. Primer sequences for qPCR.

added to 25 µL of primary antibody conjugated to magnetic microspheres and incubated overnight at 4 °C. After incubation, each well was triple-washed and incubated for 1 h with secondary antibodies. Lastly, the streptavidin/phycoerythrin was added and incubated for 30 min after further washings. All samples were run in duplicates. A Bio-Plex plate reader (Bio-Rad) was used to read the 96-well plates following a proper gating to read cytokines of interest. A standard curve for all the cytokines was prepared using the standard cytokines, and the concentrations detected in the samples were expressed as pg/mL.

Nitrite assay
For the nitrite assay, 50 µL of serum sample was added to each well of a 96-well plate, followed by adding an equal volume of Griess reagent to each well. The mixture was then incubated for 10 at room temperature. Post incubation, the colorimetric changes were measured at an absorbance of 540 nm using the Synergy 2 multi-mode microplate reader (BioTek Instruments, USA). A calibration curve was determined using standard solutions, which were used to calculate the nitrate concentrations in the samples based on the optical density measured at 540 nm wavelength. Data was presented as mean ± SEM.

ROS assay
The dichlorodihydrofluorescein (DCF) ROS/RNS Assay Kit, suitable for biofluids, culture supernatant, and cell lysates (Abcam; Catalog#ab238535), was used to measure the levels of reactive oxygen species (ROS) in serum samples. The assay was conducted per the guidelines of the manufacturer. To quantify the ROS in the samples, their fluorescence values were compared against a pre-established H_2O_2 standard curve, with measurements taken at an excitation wavelength of 480 nm and an emission wavelength of 530 nm using the Synergy 2 multi-mode microplate reader (manufactured by BioTek Instruments, USA). The results were expressed as relative fluorescence units (RFUs).

Quantification of histopathological changes in the liver and kidney
Following perfusion, the liver and kidney tissue blocks were post-fixed in 4% paraformaldehyde for 24 h, then submerged in 25% sucrose phosphate-buffered saline (PBS) for at least 3 days at 4 °C. Subsequently, the tissues were encased in a gelatin matrix (comprising 15% Type A Porcine gelatin, 7.5% sucrose, and 0.1% sodium azide in PBS, procured from Sigma, MO, USA) and maintained at 37 °C for 3 h before refrigerated overnight at 4 °C. Post refrigeration, the gelatin-encased tissues were quickly frozen using liquid nitrogen-chilled 2-methyl butane. The solidified blocks were sectioned into 5 µm using a ThermoFisher cryostat, following the methodology outlined in our prior study[27]. We collected five sections on each slide, pre-coated with chrome alum gelatin from Pfalz and Bauer, CT, USA, and stored at − 20 °C. Five sections from each organ per animal were processed for Hematoxylin and Eosin (H&E) staining. H&E stained sections were evaluated, and photomicrographs were taken using an Olympus BX43 trinocular microscope equipped with a DP27 camera and CellSens Standard Software (Olympus Corporation). A Board-certified veterinary anatomic pathologist (TA Harm) evaluated tissue using a histopathologic scoring (HS) system with five independent scoring parameters. The parameters were inflammation, tissue change (necrosis, proliferation), edema, hemorrhage, and extra-medullary hematopoiesis. A few artifacts were identified and excluded from the scoring. Artifact observations are provided in Supplementary Table S3. Each parameter was scored on a scale ranging from 0 to 5, which indicated the percentage of tissue affected (Table 4). The final cumulative score from all parameters indicated the degree of pathological change in the tissue (Table 5).

Statistical analysis
We consulted a Biostatistician, Dr. Wang, College of Veterinary Medicine, Iowa State University, for the experimental design and statistical analyses for this study. The samples were randomized, and experimental

Score	Tissue affected
0	No tissue affected
1	1–15%
2	16–30%
3	31–45%
4	46–60%
5	> 60%

Table 4. Criteria for histological evaluation.

Final interpretation (total potential score = 29)	
0–5	None to minimal change
6–10	Mild change
11–15	Moderate change
16–20	Moderate to severe change
21–29	Severe change

Table 5. Final interpretation based on total histopathological score.

groups were blinded until the data analysis was completed. We used GraphPad Prism 10.0 for statistical analysis. Robust Estimation of Outlier (ROUT) was performed wherever applicable. Normality tests were performed using the Shapiro–Wilk test paired with Q–Q plots to assess normality subjectively. Based on the normality of the data, an unpaired t-test or Mann–Whitney test was performed to compare data between the two groups. For determining interactions between sex and treatment, we performed two-way ANOVA paired with appropriate post-hoc tests for multiple comparisons between groups to remove any bias. If the interaction effects were significant, the data were presented as separate sex cohorts with relevant post hoc tests for multiple comparisons. Otherwise, the data was pooled together. In the case of histology data (Fig. 11), we presented separate images for males and females because histological images cannot be physically combined while maintaining their individual interpretability. To ensure consistency and facilitate comparison between the visual data (images) and their respective quantification, we also displayed the quantitative analysis separately for males and females despite no statistically significant sex differences. This approach was intended to maintain transparency and align the visual data presentation with quantitative results. Data in this manuscript was either presented as Cohen's d effect size[31] in Fig. 7 or Mean ± SEM in the rest of the figures.

Rigor, sample size, and inclusion or exclusion criteria

All animals used in this study were purchased from the same source (Charles River, USA). Animals were first randomized, ignoring sex, stage of the estrous cycle, and body weight. Age and sex-matched controls and SE severity-matched soman-exposed groups were blinded. The sample size and the power were determined based on our previous OPNA study outcomes from gliosis and neurodegeneration parameters[2] at a 95% confidence interval. Animals that did not reach the set SE severity score limit (> 20 min of SE), as described in our previous publications[3,26] or that did not survive the soman exposure (132 μg/kg, s.c. $1.2 \times LD_{50}$) were excluded from the study. The animals suspected of being mis-dosed were also excluded from the study. Following soman exposure, if there was a significant weight loss > 20% of total body weight in 3–4 days or the animal exhibited clear signs of distress (e.g., pain behaviors, lack of grooming, or motor impairments) were euthanized and excluded from the study. We excluded three female rats that died post-exposure based on these predetermined criteria.

Results

Soman-exposed rats had comparable initial SE severity in both sexes and all developed epilepsy

Following acute exposure to soman, all animals, irrespective of sex and the stages of estrous cycle, developed SE (> 40 min) (Fig. 2a). At the end of the study (18 weeks post-exposure), SE-matched animals were randomly selected for fresh tissue collection without perfusion [not perfused (NP)] or perfused (P) with 4% paraformaldehyde for histological examination. Most of the animals in the NP group (7 out of 10) and the P group (8 out of 10) developed handling-induced seizures in the acute phase (days 2–15 post-exposure; Fig. 2b). Continuous vEEG of P group 10–18 weeks post-exposure, confirmed that all rats developed SRS/epilepsy (Fig. 2c). There were no significant differences in SE severity and number of animals having handling induced seizures between NP and P groups (Fig. 2a,b). There were no sex differences in any of these parameters tested.

Acute soman exposure increased pro-inflammatory cytokine/chemokine gene expression 18 weeks post-exposure

qPCR analysis of isolated mRNA from the cortical brain homogenates revealed a significant change in proinflammatory cytokines. Compared to control animals, soman exposure induced a significant increase in
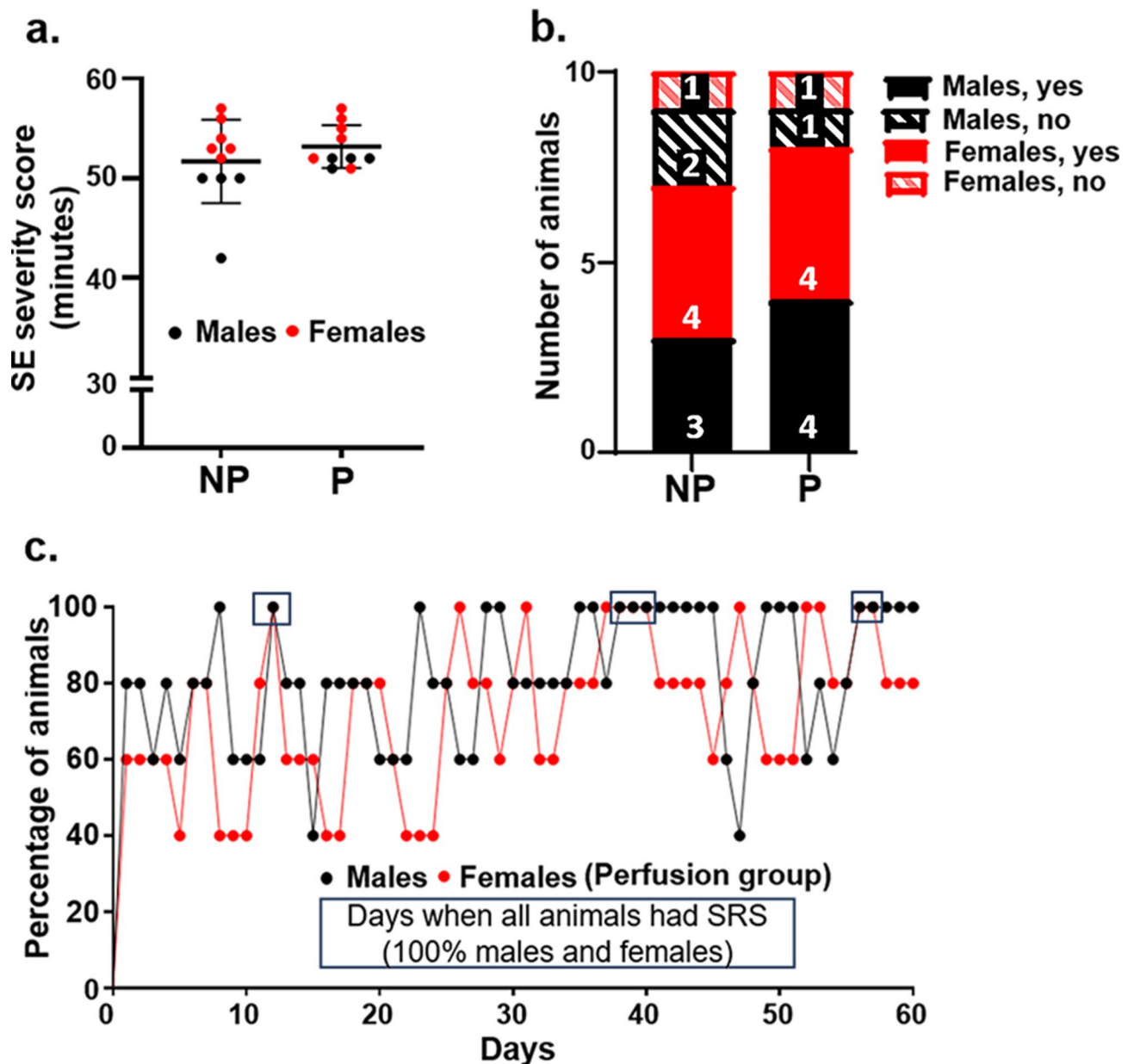
Fig. 2. Development of *status epilepticus* (SE), handling-induced seizures and spontaneously recurring seizures following acute soman exposure. Following acute soman exposure, non-perfused (NP) and perfused (P) rats were observed for initial SE and seizure development. The severity of status epilepticus (SE) in soman-exposed rats from both the NP and P groups is shown as a mixed-sex cohort (**a**). All rats in the NP and P groups (10 per group) were monitored for handling-induced seizures over 14 days (days 2–15 post-soman) (**b**). In panel (**b**), the number of male rats with and without seizures is indicated by solid black and black stripes, respectively. In contrast, the number of female rats with and without seizures is indicated by a solid red or red stripe, respectively. Continuous vEEG monitoring of P group soman rats to track SRS. The percentage of male and female rats with SRS on a particular day is shown on a 60-day timeline (**c**). In panel (**c**), the days when all 10 rats (5 males and 5 females) experienced SRS are highlighted within a box. Normality was assessed with the Shapiro–Wilk Test, n = 10 (5/sex); no significance vs control by Unpaired t-test.

mRNA expression of TNF-α (Fig. 3a), IL-6 (Fig. 3b), IL-17A (Fig. 3c), MCP-1 (Fig. 3d), IL-18 (Fig. 3e), and a chemokine IL-1α (Fig. 3f) at 18 weeks post soman exposure.

Acute soman exposure elevated pro-inflammatory cytokine/chemokine protein levels in CSF and serum at 18 weeks post-exposure

CSF and serum samples from rats were collected and processed for multiplex analysis. At 18 weeks post-exposure, CSF analysis demonstrated a significant increase in the levels of TNF-α, IL-6, IL-17A, MCP-1, IL-18, and IL-1α in soman-exposed rats compared to controls (Fig. 4a). Similarly, serum from soman exposed rats also
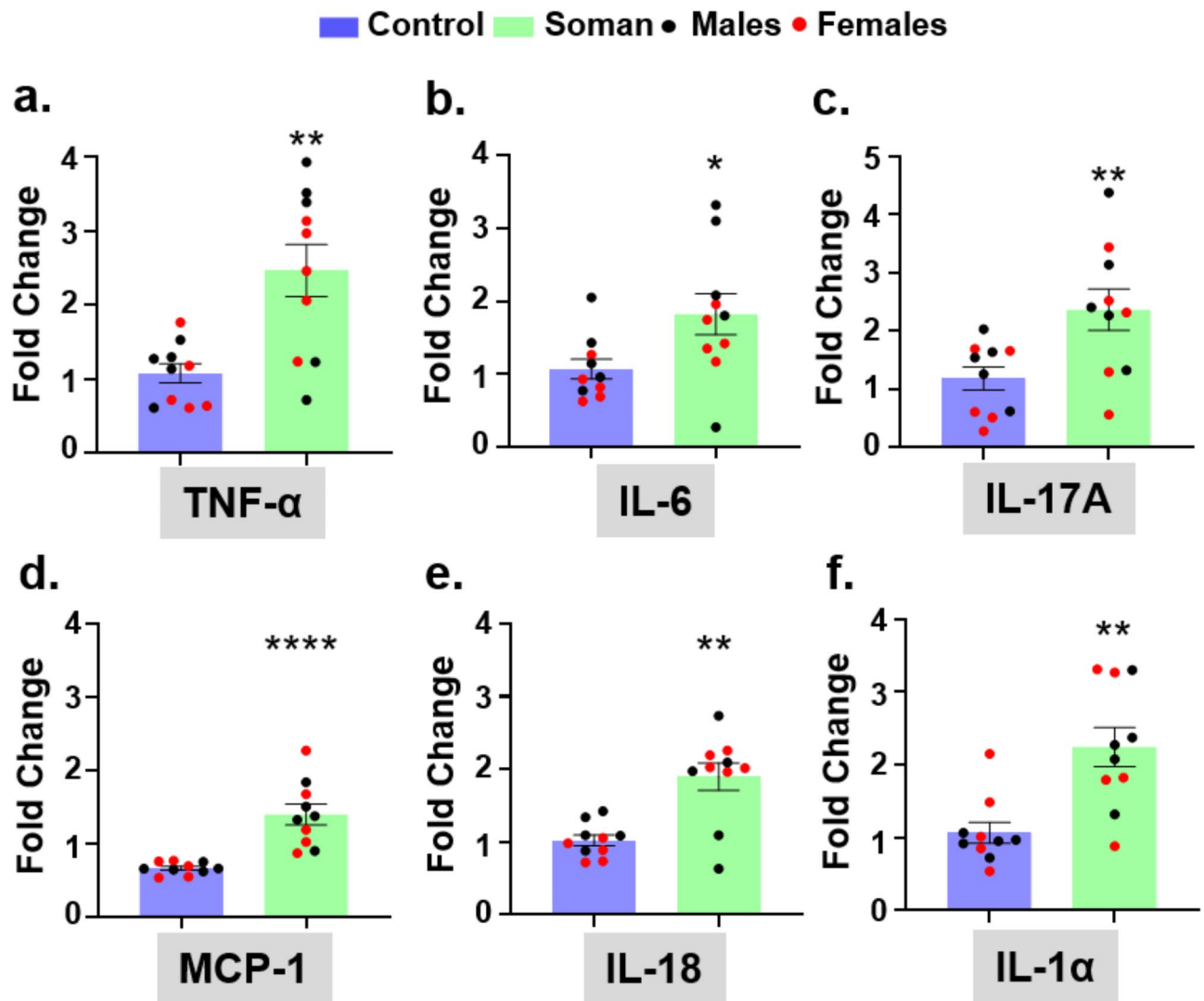
Fig. 3. Pro-inflammatory cytokine/chemokine gene expression in the rat brain (cortex) at 18 weeks post-soman exposure. mRNA was isolated from the cortex and processed for expression profile following a qPCR reaction. Gene-specific primers were used for each cytokine/chemokine and the mRNA expression levels were plotted as a fold change compared to control. Fold changes in mRNA expression for TNF-α (**a**), IL-6 (**b**), IL-17A (**c**), MCP-1 (**d**), IL-18 (**e**), and IL-1α (**f**) are shown. Normality was assessed with the Shapiro–Wilk test. Bars represent mean ± SEM, n = 10 (5/sex). *$p < 0.05$, **$p < 0.01$, ****$p < 0.0001$ versus control by Unpaired t-test (**a**–**d**) and **$p < 0.01$ vs control by Mann–Whitney test (**e**–**f**). No sex differences were observed, and data was pooled together.

demonstrated a significant increase in the levels of TNF-α, IL-6, IL-17A, MCP-1, IL-18, and IL-1α compared to controls (Fig. 4b). Notably, the levels of these proinflammatory cytokines were significantly higher in the cerebrospinal fluid (CSF) than in the serum.

Elevated pro-inflammatory cytokine/chemokine levels in the brain, CSF, and serum significantly correlated to each other at 18 weeks post-exposure
Proinflammatory cytokine/chemokine gene expression in the brain showed a significant positive correlation with the elevated levels of all cytokine/chemokine proteins detected in the CSF and serum (Fig. 5a–f).

Acute soman exposure elevated reactive oxygen/nitrogen species levels in serum, 18 weeks post-exposure
Serum samples from rats were collected and processed for serum nitrite (RNS indicator) and reactive oxygen species (ROS) 18 weeks post-exposure. Serum analysis demonstrated a significant increase in the levels of serum nitrite (Fig. 6a) and reactive oxygen species (ROS) (Fig. 6b).
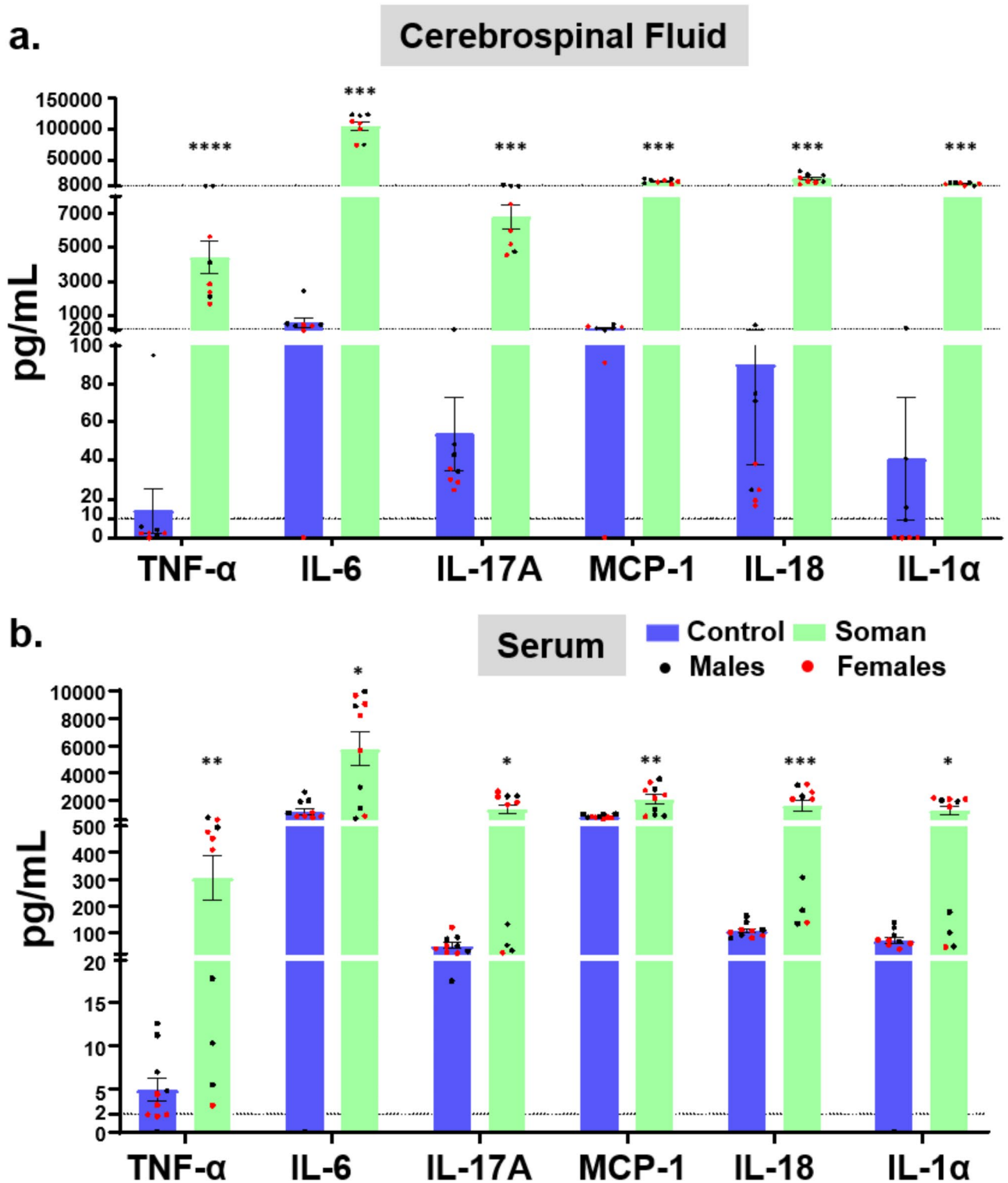
Fig. 4. Secreted pro-inflammatory cytokine/chemokines in the CSF and serum of the rats at 18 weeks post-soman exposure. A customized MILLIPLEX® Rat Cytokine/Chemokine kit was used to analyze each cytokine/chemokine. The results are plotted as pg/mL of CSF (**a**) or serum (**b**) for TNF-α, IL-6, IL-17A, MCP-1, IL-18, and IL-1α. Normality was assessed with the Shapiro–Wilk test. Bars represent mean ± SEM, n = 10 (5/sex) for serum and n = 8 (4/sex) for CSF. **$p < 0.01$, ***$p < 0.001$ versus control by Unpaired t-test (MCP-1) and *$p < 0.05$, **$p < 0.01$ and ***$p < 0.001$, ****$p < 0.0001$ versus control by Mann–Whitney test (TNF-α, IL-6, IL-17A, IL-18, and IL-1α). No sex differences were observed, and data are presented as mixed-sex cohort.
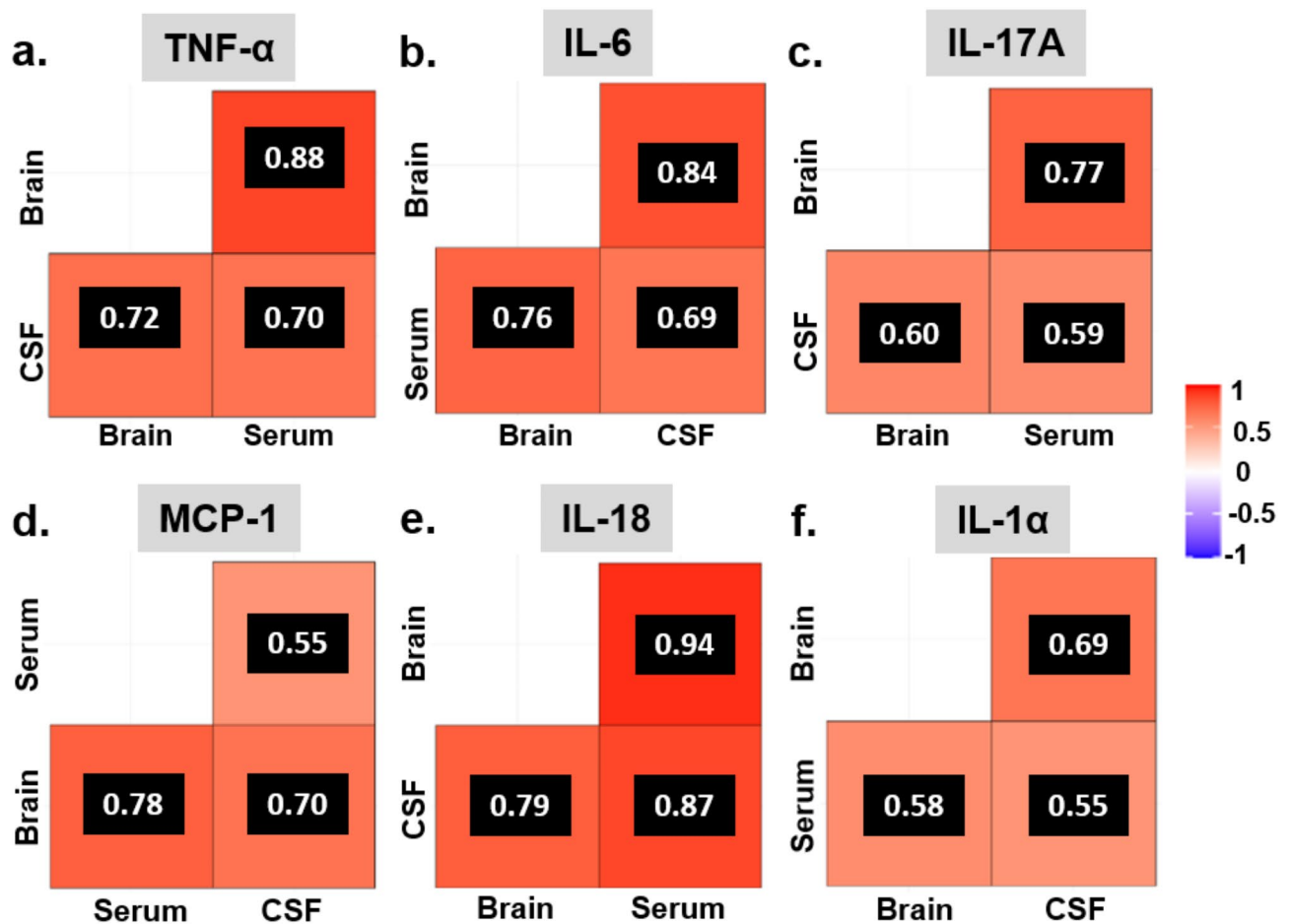
Fig. 5. Correlational profile of pro-inflammatory cytokine/chemokine in the brain, CSF, and serum. Correlation matrices of TNF-α, IL-6, IL-17A, MCP-1, IL-18, and IL-1α for CSF (**a**–**f**) between brain genes expression, secreted proteins in CSF and serum (**a**–**f**). Normality was assessed with the Shapiro–Wilk test. Values represent the correlation coefficient (center of each matrix square), n = 8 (4/sex). $p < 0.05$ versus control by Spearman correlation analysis (color represents strength and direction of correlation). No sex differences were observed, and data was pooled together.

Acute exposure to soman-induced neurobehavioral changes at 4–8 weeks post-exposure

Neurobehavioral analysis of mixed-sex cohorts was conducted during 4–8 weeks post-exposure. Cohen's d effect size analysis detected the effect size between soman-exposed and control rats in recognition and contextual/cued memory. A large negative effect in the novel object recognition test suggested a significantly poorer recognition memory in soman-exposed rats compared to control rats [Cohen's d = − 1.42; 95% CI (− 2.26, − 0.47), $p = 0.0001$] (Fig. 7a). A large negative effect in contextual/cued memory performance [Cohen's d = − 1.13; 95% CI (− 1.70, − 0.50), $p = 0.0004$] indicated that soman-exposed rats performed significantly worse on contextual/cued memory compared to control rats (Fig. 7b).

Acute exposure to soman did not change hematological parameters at 18 weeks

A comprehensive hematological analysis indicated no significant differences in the red blood cell count, reticulocyte count, hematocrit levels, hemoglobin concentration, mean corpuscular volume (MCV), mean corpuscular hemoglobin (MCH), mean corpuscular hemoglobin concentration (MCHC), red cell distribution width (RDW), and platelet cell count between the soman-exposed and the control groups (Fig. 8a). A similar trend was observed in white blood cells including neutrophils, lymphocytes, monocytes, eosinophils, and basophils. No significant differences existed between the group exposed to soman and the control group (Fig. 8b).

Soman exposure increased total bilirubin levels without affecting AST and ALT at 18 weeks post-exposure

Biochemical analysis of the serum demonstrated a significant increase in total bilirubin levels (Fig. 9a). However, no significant changes were observed in the serum Alanine Aminotransferase (ALT) (Fig. 9b) and Aspartate Aminotransferase (AST) levels (Fig. 9c) to soman exposure when compared with control animals.
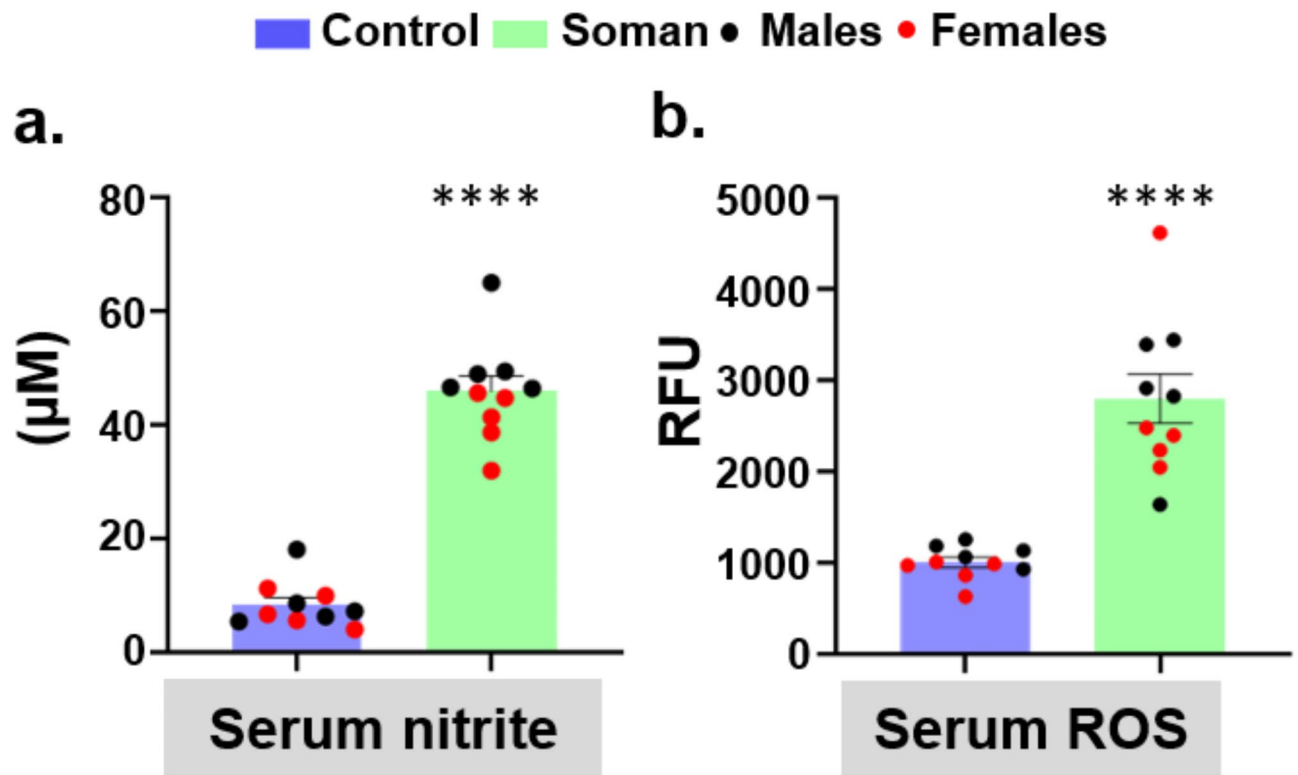
Fig. 6. Secreted RNS and ROS in the rat serum following soman exposure. Griess Nitrite Assay Kit and ROS Assay Kit were used to determine their concentrations in serum. The results are plotted as µM for serum nitrite (**a**) and relative fluorescence units (RFU) for ROS (**b**). Normality was assessed with the Shapiro–Wilk test. Bars represent mean ± SEM, n = 10 (5/sex); ****$p < 0.0001$ versus control by Unpaired t-test (**a**,**b**). No sex differences were observed.
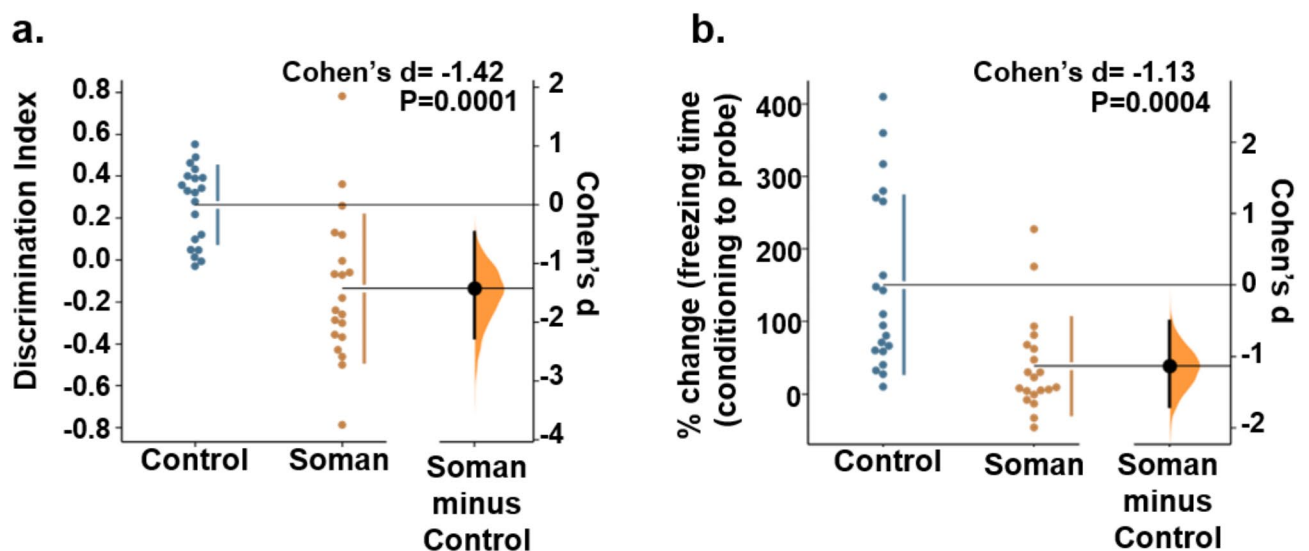

Fig. 7. Effect size analysis of neurobehavioral outcomes following soman exposure. Results from recognition memory (week 5 post soman) (**a**) and contextual/cued memory (week 7 post soman) (**b**) are shown. Cohen's d effect size analysis showed a significant difference in soman-exposed animals compared to control animals. Normality was assessed with the Shapiro–Wilk Test, n = 40 (20/sex); significant effect size in soman minus control by Cohen's d test.
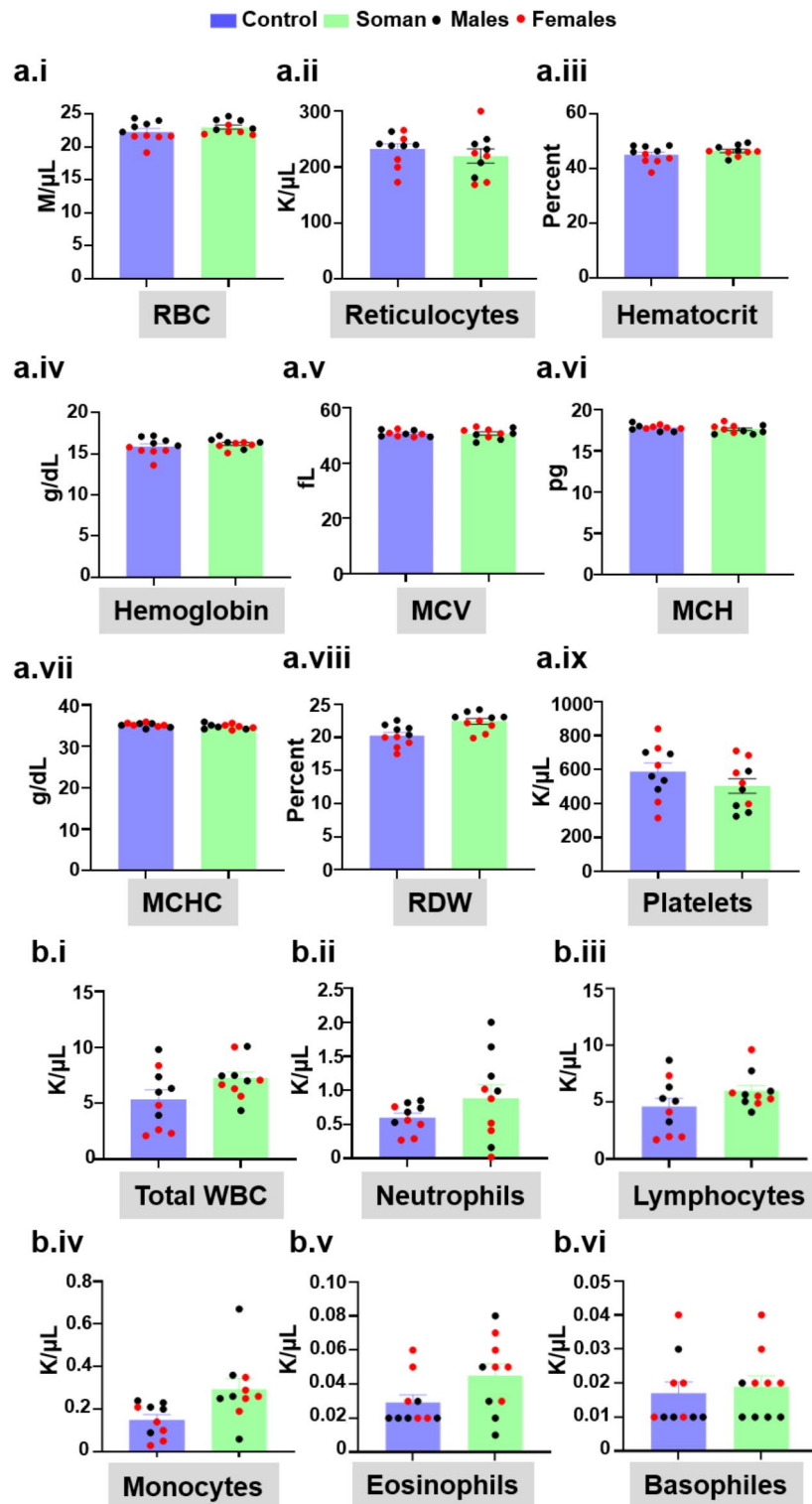
Fig. 8. Hematological parameters at 18 weeks post-soman exposure. Whole blood was analyzed for various hematological parameters like RBC count, reticulocytes, hematocrit, hemoglobin, MCV, MCH, MCHC, RDW, and platelets (**a**). Total WBC and various WBCs like neutrophils, lymphocytes, monocytes, eosinophils, and basophils were counted in the whole blood of rats (**b**). The results are plotted as millions of cells/μL (RBC), thousands of cells/μL (Reticulocytes, Platelets, Total WBC and various WBCs like neutrophils, lymphocytes, monocytes, eosinophils, and basophils), Percent (Hematocrit and RDW), gram/dL (Hemoglobin and MCHC), MCV (femtoliters), and picogram (MCH). Normality was assessed with the Shapiro–Wilk test. Bars represent mean ± SEM, n = 10 (5/sex); no statistical significance between soman and control by Unpaired t-test (**a,b**). No sex differences were observed.
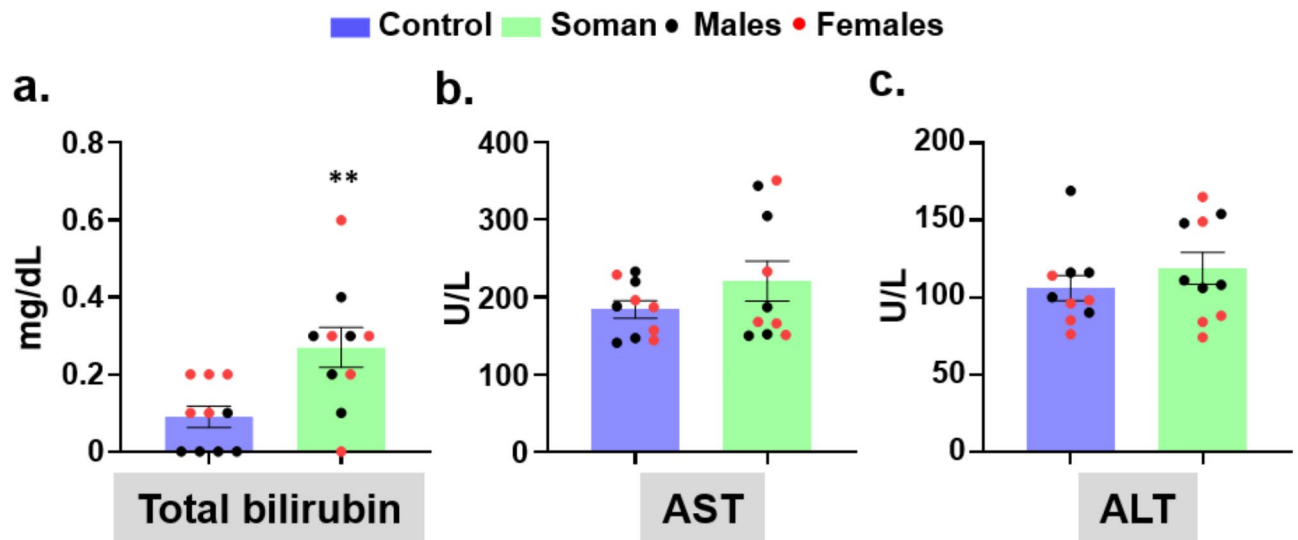
Fig. 9. Liver function tests at 18 weeks post-soman exposure. Total bilirubin levels in serum were significantly upregulated in soman-exposed animals compared to control (**a**). However, there were no significant differences in the AST (Aspartate Aminotransferase) (**b**) and ALT (Alanine Aminotransferase) (**c**) levels between the groups. Normality was assessed with the Shapiro–Wilk test. Bars represent mean ± SEM, n = 10 (5/sex). **$p < 0.01$ soman versus control by Mann–Whitney test (**a**). No sex differences were observed.
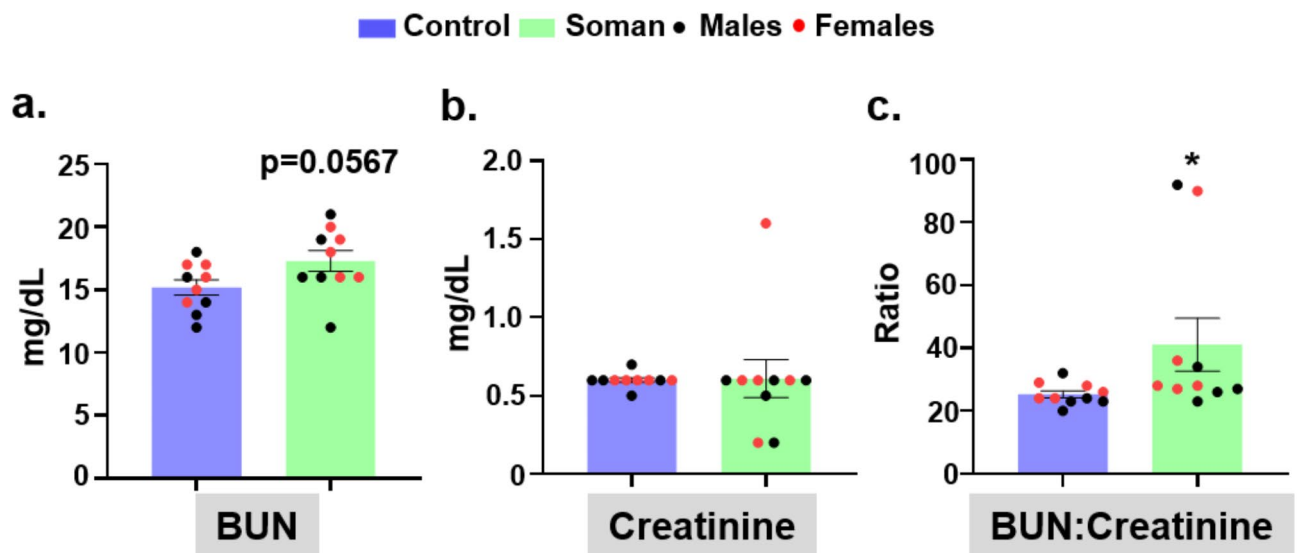
Fig. 10. Kidney function tests at 18 weeks post-exposure. Serum values of BUN (**a**), creatinine (**b**), and BUN to creatinine ratio (**c**) at 18 weeks following soman exposure are shown. Normality was assessed with the Shapiro–Wilk test. Bars represent mean ± SEM, n = 10 (5/sex). $p = 0.0567$ versus control by Unpaired t-test (**a**), no significance vs control by Mann–Whitney test (**b**) and *$p < 0.05$ vs control by Mann–Whitney test (**c**). No sex differences were observed.

Soman exposure increased BUN levels but not creatinine at 18 weeks post-exposure
BUN and creatinine levels in the serum were measured to assess kidney function. The BUN-to-creatinine ratio was subsequently calculated for each sample. At 18 weeks post-soman exposure, BUN levels increased compared to control (Fig. 10a). However, the differences were not statistically significant ($p = 0.0567$). In contrast, creatinine levels remained unchanged in both groups (Fig. 10b). The BUN-to-creatinine ratio was significantly elevated in soman-exposed animals compared to controls (Fig. 10c).

Histopathology revealed no significant morphological changes in the liver or kidney at 18 weeks post-soman exposure

Hematoxylin and Eosin stained liver and kidney sections were examined microscopically to screen for evidence of morphological changes associated with soman exposure. Focal inflammation artifacts in the liver and kidney were observed in both control and soman-exposed tissues with no statistically significant differences, details in Supplementary Table S3. Since the signs of tissue necrosis, edema, or hemorrhage were not found in either group, no scores were given in these parameters. The total histopathological scores (HS) only accounted for focal inflammation (e.g., score 1, mononuclear cells, and few neutrophils) and extra-medullary hematopoiesis (EMH) (e.g., score 1, bi- to tri-lineage development). Details of individual scores are provided in (Supplementary Tables S4 and S5). Representative H&E stained tissue section photomicrographs from the liver and kidney are shown in Fig. 11a–h. In summary, histopathologic examination of liver and kidney sections did not reveal changes consistent with toxicity, inflammation, or necrosis in response to soman exposure Fig. 11i–l.

Discussion

Acute exposure to OPNAs has been known to cause classical cholinergic symptoms such as salivation, lacrimation, urination, defecation (SLUD), and seizures that can be controlled with atropine, oxime, and anti-seizure medication, and these could also prevent death if administered soon after exposure[32–34]. However, delayed treatment could prolong seizures and cause brain injury in the long term despite treating with symptomatic drugs[35]. Experimental models of OPNA have confirmed that most animals that had seizures for >20 min develop spontaneous seizures[3,36]. The occurrence of spontaneous seizures likely contributes to a vicious cycle of neuroinflammatory and nitro-oxidative stressors, as seizures can activate microglia and astrocytes (resident immune cells in the brain), leading to the release of pro-inflammatory cytokines and reactive oxygen/nitrogen species locally in the brain[2,37,38]. This increased production of proinflammatory cytokines and chemokines can also be detected in CSF and serum[3,9,39]. These inflammatory mediators, in turn, exacerbate neuronal excitability and disrupt homeostasis, further promoting seizure recurrence, a phenomenon described as "seizure-begets-seizure". This bidirectional interplay highlights the critical role of neuroinflammation and oxidative stress in perpetuating epileptogenesis and worsening disease progression and associated comorbidity and pathology.

We previously showed serum biomarkers in another OPNA model (DFP) at 6 weeks post-exposure in a rat model[16]. In the rat soman model, we recently demonstrated brain structural and functional MRI changes that correlated with behavioral dysfunction and neuroinflammatory changes[40]. Also, the brain histological changes, such as reactive gliosis and neurodegeneration at 18 weeks post-soman, confirmed the brain MRI changes observed at 10 weeks post-exposure[3]. In this study, the serum and CSF from the same animals used for neurobehavior testing, SRS, and histology revealed a significant increase in proinflammatory cytokines, chemokines, and nitro-oxidative stressors, implying brain inflammation. While these readouts are robust and reliable for OPNA-induced long-term effects, behavioral testing of a large human population post-exposure can be expensive and impractical. Moreover, unlike in the experimental model, brain histology is not possible. While serum cytokines and oxidative stress analysis can be routinely performed, it does not differentiate between central and peripheral toxicity. This study aims to extend our previous work to understand the source of chronic biomarkers and build upon it by investigating the source of chronic biomarkers, determining whether they originate centrally or peripherally. Additionally, it examines whether these centrally produced biomarkers influence neurobehavioral outcomes and impact the function of vital organs such as the liver and kidneys. Therefore, we performed a comprehensive hematological/biochemical analysis of the blood, cognitive behavioral studies, SRS profile, and inflammatory marker analyses in CSF, serum, and brain to investigate this complex interplay. Currently, such integrated analysis of the long-term effects of acute exposure to soman is lacking, and this study addresses this significant gap in our understanding of OPNA-induced chronic toxicity.

Previously, there have been studies to identify potential biomarkers post OPNA exposure, such as AChE/BChE concentrations in RBC, OPNA levels in the serum or plasma, or its metabolites in urine[41,42]. However, these tests are appropriate for a couple of hours or days after acute exposure to OPNA. Some studies suggest that biomonitoring of protein adducts using immune sensors may detect a low-level exposure within hours to a couple of days[43]. In a recent study of VX exposure on rats, a serum albumin adduct, Cys^{34}(-DPAET)Pro, was detected in in-vivo specimens and showed a time-dependent concentration increase after subcutaneous exposure in rats[44]. Since the average half-life of soman is about 9 h[45] and it gets cleared from the body within a couple of days in humans, there are no biomarkers to detect soman-induced effects beyond this point. Furthermore, considering rat's high basal metabolic rate[46,47], OPNA clearance is even faster. While studies on organophosphate pesticides have provided insights into their chronic effects, the higher potency and distinct pharmacokinetics of OPNAs like soman may lead to different long-term outcomes. Our findings contribute to the broader understanding of AChE-inhibiting agents by elucidating the specific chronic effects of soman, thereby informing medical countermeasures and therapeutic strategies tailored to nerve agent exposures.

Previous studies have only investigated the early time points with subclinical doses of soman[17]. A marked decrease in red blood cell counts and hematocrit levels was observed, suggesting increased hemolysis in rabbits exposed to a low dose of soman (50 μg/kg). The blood parameters were analyzed in the rabbit study at 1, 2, 4, 24, and 48 h post-exposure. A substantial decline in cholinesterase levels, while an increase in creatinine phosphokinase activity was noticed at specific doses in the rabbit model. In the mouse model, low to moderate doses of soman (30–90 μg/kg) demonstrated reduced central cholinesterase activities, which impacted motor function in a dose-dependent manner at 30 min, 24 h, and 7 days after poisoning[17,19].

Contrary to previous studies, we evaluated the prolonged effects of a substantial dose of soman ($1.2 \times LD_{50}$) for robust SRS development, neurobehavior deficits, proinflammatory cytokines, nitro-oxidative stress, and significant impairment of liver and kidney functions. Furthermore, we also reported the long-term effects of
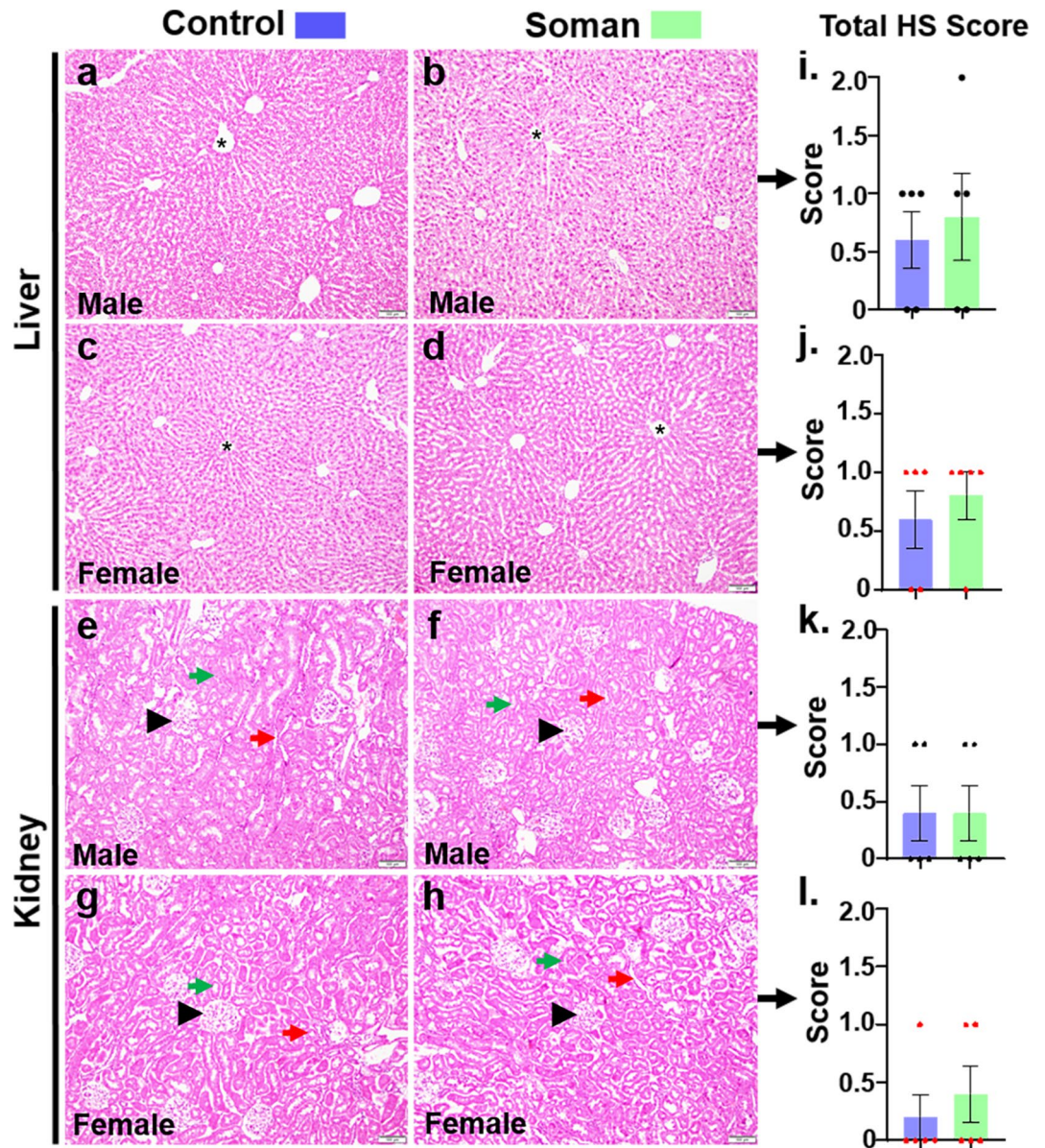
Fig. 11. Microscopic anatomy of liver and kidney from control and soman exposed rats. Representative photomicrographs of the liver sections from male (**a,b**) and female (**c,d**) rats that were exposed to soman (**b,d**) or vehicle (**a,c**) are shown. The images highlight one or more hepatic lobules with the central vein indicated by the star (*). Histopathologic examination of the liver sections did not identify significant microscopic changes associated with soman. Representative photomicrographs of the kidney sections from male (**e,f**) and female (**g,h**) rats that were exposed to soman (**f,h**) or vehicle (**e,g**). The images highlight the glomeruli (arrowheads), the proximal convoluted tubules (green arrows), and the distal convoluted tubules (red arrows). Histopathologic examination of the kidney sections did not identify any significant microscopic changes associated with soman and had no differences in the final total HS (**i–l**). Normality was assessed with the Shapiro–Wilk test. Bars represent mean ± SEM, n = 10 (5/sex); scale bar = 100 μm. no significance vs control by Mann–Whitney test (**i–l**). No sex differences were observed, and data was not pooled to complement images (**a–h**).

soman on routine blood parameters. Such comprehensive evaluations can be helpful in assessing the efficacy of therapies.

We have previously demonstrated a significant increase in serum cytokines and nitrite levels at 1 week, 2 weeks, and 6 weeks post-exposure in the rat DFP model, a surrogate for soman[48]. In a soman rat model, we found a significant upregulation of cytokines and nitrite levels at 18 weeks post-exposure, validating the cytokines and nitrite upregulation in OPNA models at chronic time points. However, in those studies, there was no evidence of the source of the cytokines and nitro-oxidative stress markers. In this study, we demonstrate that their production was from the brain but not from the circulating leukocytes, as evident from the concomitant

increase in their gene expression (Fig. 3). Immunohistochemistry of brain sections for reactive glia markers (IBA1 + CD68 for reactive microgliosis and GFAP + C3 for reactive astrogliosis) and, inducible nitric oxide synthase (iNOS) suggested a significant increase of these markers in OPNA exposed animals at various time-points[3,16,48].

Reactive glial cells are known to produce proinflammatory cytokines and chemokines[49–51] with a simultaneously increasing gene transcription[52,53]. Microglia are the sensors of changes in the CNS microenvironment and are known to regulate the innate immune responses of astrocytes via microglia-astrocyte crosstalk[54]. The astrocytes also form intimate connections with neurons and blood vessels. Thus, they can detect neuronal damage and effectively regulate inflammatory responses by modulating microglia[54,55]. Reactive astrocytes also produce MCP1, which acts on CCR2 receptors expressed by stressed neurons and reactive microglia. The elevated gene expression of proinflammatory cytokines in the brain and the increase in cytokine levels in the CSF and serum imply that the source of inflammation is likely central rather than peripheral. The lack of significant changes in systemic hematological parameters in response to soman exposure further supports this finding. In a previous study, co-labeling of IBA1 with iNOS and NeuN with 3NT in brain sections suggested reactive glia indeed upregulated iNOS, produced reactive nitrogen species, and nitrosylated proteins on their tyrosine residues (3NT) in neurons[16]. Since the peripheral leukocyte counts or the ratio of various cell types did not change in soman-exposed animals compared to controls, it is likely that the nitro-oxidative stress markers also originated from the brain in soman-exposed animals.

A comprehensive study of the adult population in the US by the National Health and Nutrition Examination Survey (NHANES) found that exposure to OP pesticides is significantly associated with liver injury or liver function biomarkers[56]. There is also evidence suggesting that long-term exposure to organophosphate pesticides might lead to subclinical liver damage severe enough to affect liver function[57]. Total bilirubin, a byproduct of the breakdown of red blood cells, is an essential marker of liver function. This study found elevated total bilirubin levels at 18 weeks post-exposure, a significant indicator of hepatic dysfunction and suggests potential hepatotoxic effects of soman. Thus, monitoring total bilirubin levels in individuals exposed to organophosphates is clinically relevant. Elevated levels of ALT and AST in the blood indicate liver inflammation or altered liver function[14]. At the 18-week post-exposure to soman, animals showed stable serum ALT and AST levels, indicating that long-term liver function may not be severely affected by soman at the time point tested. The liver histology corroborated the serum biomarker findings, showing no significant pathological alterations in the soman-exposed group at 18 weeks. However, total bilirubin levels in soman-exposed rats approached the higher end of the normal range and were markedly elevated compared to the control group. This trend raises concerns and underscores the importance of monitoring, as total bilirubin could potentially serve as an early indicator of soman toxicity in chronic phase. These findings suggest that functional impairments typically precede histological microscopic changes, given the significant rise in total bilirubin levels in the soman-exposed subjects.

The pathogenesis of renal injury due to OPNA intoxication remains largely unknown, but the damage likely occurs at the renal tubules[58]. Experimental and clinical studies have also revealed that exposure to organophosphate flame retardants (OPFRs) is associated with renal tubular toxicity and renal impairment[59]. BUN and creatinine levels are vital parameters for assessing the health of the kidney[15,60]. At 18 weeks post-exposure, a consistent rise in serum blood urea nitrogen (BUN) levels ($p = 0.0567$) and a significantly higher BUN to creatinine ratio were observed. In contrast, serum creatinine levels remained unchanged, and kidney histology showed no detectable abnormalities at cellular level. These findings suggest early functional renal changes without overt structural damage. Elevated BUN and the BUN to creatinine ratio without corresponding histological alterations may indicate early functional impairment that precedes structural changes, reflecting stress on kidneys or reduced efficiency[61]. One plausible explanation is pre-renal azotemia, where decreased renal perfusion leads to elevated BUN levels without intrinsic kidney damage, consistent with the normal histological findings[62]. Additionally, traditional histological methods like H&E staining may not detect subtle molecular or early-stage structural changes, as functional impairments can occur without visible cellular alterations. This underscores the need to integrate biochemical assessments with more sensitive histological techniques to understand renal health comprehensively. These findings highlight the importance of monitoring functional biomarkers to detect early renal changes, which may have significant implications for long-term kidney function in survivors.

The findings from this study underscore the importance of monitoring the biological parameters that may manifest over an extended period post-soman exposure. While the study indicates that soman exposure does not significantly alter specific blood hematological parameters in rats, the increase in serum total bilirubin and BUN to creatinine ratio is intriguing. These hepatic and renal alterations warrant further investigation into how soman exposure might affect organ functions over time. The absence of significant hematological changes post-exposure suggests that the inflammatory biomarkers originated from brain inflammation due to SRS-induced effects and these cytokines in turn may have impacted systemic changes. In this study, we found that all perfused soman-exposed animals developed epilepsy and had several spontaneous seizures during 10–18 weeks post-exposure (Fig. 2). Seizures are known to increase brain inflammation[3,16]. Furthermore, detecting high levels of secreted cytokine proteins in the CSF and a significant increase in the brain mRNA strongly supports that the increased cytokines observed in serum originated from seizure-induced effects in the brain. Correlation analysis confirmed a positive correlation between secreted cytokine proteins in CSF, serum, and brain mRNA for cytokines. The absence of a broad peripheral immune response in this study aligns with soman's known mechanism of action, primarily due to seizure-inducing effect of OPNAs in the brain rather than the peripheral immune system in chronic stage[2]. Gut inflammation can occur in response to acute exposure to AChE inhibitors if there is a systemic circulation of active AChE inhibitors or their metabolites[63]. However, gut inflammation is unlikely to persist for 18 weeks post-exposure. Indeed, we have demonstrated the impact of acute exposure to DFP (AChE inhibitor) on the gut microbiome, which altered in response to gut inflammation at 2 and 7 days

but not at 5 weeks post-exposure[64], implying that systemic effects of AChE inhibitors are not long-lasting. Therefore, the increased cytokines levels observed in this study are unlikely from the gut inflammation. Given the severity of acute soman poisoning in humans, the findings from the experimental models highlight the translational potential of this study outcomes from diagnostic and countermeasure perspectives. However, while extrapolating the results from the experimental model to humans, one should consider the physiological and biochemical differences between the species[65].

This study highlights the importance of identifying chronic biomarkers reflective of ongoing neuropathological and systemic processes, as demonstrated in the rat soman model[3]. Focusing on the chronic phase after acute effects have resolved, we identified neurobehavioral deficit and chronic biomarkers, such as elevated proinflammatory cytokines, reactive oxygen/nitrogen species, and total bilirubin, indicating chronic neuroinflammation and potential organ dysfunction without significant microscopic morphological changes. These findings emphasize the need to monitor long-term systemic and neurological effects (comorbidity), offering insight into therapeutic strategies for survivors beyond epilepsy management. While our prior studies have investigated later time points following soman exposure[2,3,40], this manuscript builds on that work by focusing on systemic-to-central interactions and neurobehavioral outcomes over a chronic timeframe. Importantly, this study integrates biochemical markers, neuroinflammation, and behavioral outcomes, providing a more comprehensive understanding of chronic soman toxicity. By elucidating the complex interplay between systemic inflammation, neuroinflammation, and behavioral deficits, this study advances our understanding of the long-term impacts of soman exposure. Furthermore, this model bridges preclinical and clinical relevance by reflecting survivors' chronic health challenges of nerve agent attacks or pesticide exposure, where acute biomarkers such as AChE/BChE assays lose utility over time. The identified chronic biomarkers fill this gap, providing biomarkers for assessing long-term health impacts and guiding targeted therapeutic interventions for survivors.

Conclusion

This study provides critical insights into the long-term effects of acute soman exposure, emphasizing the importance of identifying chronic biomarkers that reflect systemic and neuropathological changes. The findings reveal that soman exposure induces SRS, neurobehavioral deficits, chronic neuroinflammation, and subtle hepatic and renal impairments that may precede overt structural damage. Elevated proinflammatory cytokines, nitro-oxidative stress markers, and serum total bilirubin highlight the persistent impact on the brain and peripheral organs. At the same time, changes in the BUN to creatinine ratio suggest early functional renal changes despite normal histology. These biomarkers offer promising tools for assessing the long-term health impacts of soman exposure and guiding therapeutic interventions. While hematological parameters remained unchanged, the study underscores the limitations of relying solely on traditional histological methods and the need to integrate biochemical and molecular assessments to evaluate organ function comprehensively. The absence of a broad peripheral immune response aligns with soman's mechanism of action, primarily targeting the nervous system. However, the subtle yet significant changes in renal and hepatic biomarkers warrant further investigation into how soman exposure affects organ systems at even later times. These findings bridge preclinical and clinical relevance, highlighting the translational potential of this research to develop practical diagnostic tests and therapeutic strategies for survivors of nerve agent exposure. Future studies should focus on species-specific differences when extrapolating these results to humans and prioritize comprehensive approaches to monitoring chronic health impacts, particularly in cases of delayed treatment. This study advances our understanding of soman toxicity and underscores the critical need for long-term monitoring and targeted countermeasures to mitigate its chronic effects.

Data availability

The datasets used and/or analyzed during the current study are available from the corresponding author on reasonable request and can also be accessed as supplementary information files.

References

1. Department of Health and Human Sciences, C. (ed CDC) (2003).
2. Gage, M. et al. Soman (GD) rat model to mimic civilian exposure to nerve agent: Mortality, video-EEG based *status epilepticus* severity, sex differences, spontaneously recurring seizures, and brain pathology. *Front. Cell. Neurosci.* **15**, 798247. https://doi.org/10.3389/fncel.2021.798247 (2022).
3. Vasanthi, S. S. et al. Disease-modifying effects of a glial-targeted inducible nitric oxide synthase inhibitor (1400W) in mixed-sex cohorts of a rat soman (GD) model of epilepsy. *J. Neuroinflamm.* **20**, 163. https://doi.org/10.1186/s12974-023-02847-1 (2023).
4. National Research Council, Division on Earth, Life Studies, Board on Environmental Studies & Subcommittee on Chronic Reference Doses for Selected Chemical Warfare Agents. *Review of the US Army's Health Risk Assessments for Oral Exposure to Six Chemical-Warfare Agents* (1999).
5. Jackson, C., Ardinger, C., Winter, K., McDonough, J. & McCarren, H. Validating a model of benzodiazepine refractory nerve agent-induced status epilepticus by evaluating the anticonvulsant and neuroprotective effects of scopolamine, memantine, and phenobarbital. *J. Pharmacol. Toxicol. Methods* **97**, 1–12. https://doi.org/10.1016/j.vascn.2019.02.006 (2019).
6. Hulse, E., Haslam, J., Emmett, S. & Woolley, T. Organophosphorus nerve agent poisoning: Managing the poisoned patient. *Br. J. Anaesth.* **123**, 457–463. https://doi.org/10.1016/j.bja.2019.04.061 (2019).
7. Sharma, S. et al. Mechanisms of disease-modifying effect of saracatinib (AZD0530), a Src/Fyn tyrosine kinase inhibitor, in the rat kainate model of temporal lobe epilepsy. *Neurobiol. Dis.* **156**, 105410. https://doi.org/10.1016/j.nbd.2021.105410 (2021).
8. Patel, D., Tewari, B., Chaunsali, L. & Sontheimer, H. Neuron–glia interactions in the pathophysiology of epilepsy. *Nat. Rev. Neurosci.* **20**, 282–297. https://doi.org/10.1038/s41583-019-0126-4 (2019).

9. Frankola, K. A., Greig, N. H., Luo, W. & Tweedie, D. Targeting TNF-alpha to elucidate and ameliorate neuroinflammation in neurodegenerative diseases. *CNS Neurol. Disord. Drug Targets (Former. Curr. Drug Targets CNS Neurol. Disord.)* **10**, 391–403 (2011).

10. Lyra e Silva, N. M. et al. Pro-inflammatory interleukin-6 signaling links cognitive impairments and peripheral metabolic alterations in Alzheimer's disease. *Transl. Psychiatry* **11**, 251 (2021).

11. Vezzani, A., Maroso, M., Balosso, S., Sanchez, M. A. & Bartfai, T. IL-1 receptor/toll-like receptor signaling in infection, inflammation, stress and neurodegeneration couples hyperexcitability and seizures. *Brain Behav. Immun.* **25**, 1281–1289. https://doi.org/10.1016/j.bbi.2011.03.018 (2011).

12. Meyer, C. et al. The NADPH oxidase inhibitor, mitoapocynin, mitigates DFP-induced reactive astrogliosis in a rat model of organophosphate neurotoxicity. *Antioxidants* **12**, 2061. https://doi.org/10.3390/antiox12122061 (2023).

13. Greathouse, B., Zahra, F. & Brady, M. F. *Acetylcholinesterase Inhibitors Toxicity* (2018).

14. Karami-Mohajeri, S., Ahmadipour, A., Rahimi, H. & Abdollahi, M. Adverse effects of organophosphorus pesticides on the liver: a brief summary of four decades of research. *Arh. Hig. Rada Toksikol. Arch. Ind. Hyg. Toxicol.* 68, 261–275. https://doi.org/10.1515/aiht-2017-68-2989 (2017).

15. Gounden, V., Bhatt, H. & Jialal, I. *Renal Function Tests* (2018).

16. Putra, M. et al. Inducible nitric oxide synthase inhibitor, 1400W, mitigates DFP-induced long-term neurotoxicity in the rat model. *Neurobiol. Dis.* **133**, 104443. https://doi.org/10.1016/j.nbd.2019.03.031 (2020).

17. Baille, V. et al. Acute exposure to a low or mild dose of soman: Biochemical, behavioral and histopathological effects. *Pharmacol. Biochem. Behav.* **69**, 561–569 (2001).

18. Pohanka, M., Románek, J. & Pikula, J. Acute poisoning with sarin causes alteration in oxidative homeostasis and biochemical markers in Wistar rats. *J. Appl. Biomed.* **10**, 187–193. https://doi.org/10.2478/v10136-012-0010-2 (2012).

19. Lee, M. & Clement, J. Effects of soman poisoning on hematology and coagulation parameters and serum biochemistry in rabbits. *Mil. Med.* **155**, 244–249 (1990).

20. El Sayed, S. et al. A chromogenic probe for the selective recognition of sarin and soman mimic DFP. *ChemistryOpen* **3**, 142–145 (2014).

21. Rojas, A. et al. Comparison of neuropathology in rats following status epilepticus induced by diisopropylfluorophosphate and soman. *Neurotoxicology* **83**, 14–27 (2021).

22. Mukherjee, S. & Gupta, R. D. Organophosphorus nerve agents: Types, toxicity, and treatments. *J. Toxicol.* **2020**, 3007984 (2020).

23. Gearhart, J., Jepson, G., Clewell, H., Andersen, M. & Conolly, R. Physiologically based pharmacokinetic model for the inhibition of acetylcholinesterase by organophosphate esters. *Environ. Health Perspect.* **102**, 51–60 (1994).

24. Chen, K., Teo, S. & Seng, K. Sensitivity analysis on a physiologically-based pharmacokinetic and pharmacodynamic model for diisopropylfluorophosphate-induced toxicity in mice and rats. *Toxicol. Mech. Methods* **19**, 486–497. https://doi.org/10.1080/15376510903300335 (2009).

25. Rao, N. S. et al. DFP-induced status epilepticus severity in mixed-sex cohorts of adult rats housed in the same room: Behavioral and EEG comparisons. *Front. Cell Dev. Biol.* **10**, 895092. https://doi.org/10.3389/fcell.2022.895092 (2022).

26. Gage, M. et al. Differential impact of severity and duration of *status epilepticus*, medical countermeasures, and a disease-modifier, saracatinib, on brain regions in the rat diisopropylfluorophosphate model. *Front. Cell. Neurosci.* **15**, 772868. https://doi.org/10.3389/fncel.2021.772868 (2021).

27. Puttachary, S. et al. 1400W, a highly selective inducible nitric oxide synthase inhibitor is a potential disease modifier in the rat kainate model of temporal lobe epilepsy. *Neurobiol. Dis.* **93**, 184–200. https://doi.org/10.1016/j.nbd.2016.05.013 (2016).

28. Wyatt-Johnson, S. K., Sommer, A. L., Shim, K. Y. & Brewster, A. L. Suppression of microgliosis with the colony-stimulating factor 1 receptor inhibitor PLX3397 does not attenuate memory defects during epileptogenesis in the rat. *Front. Neurol.* **12**, 651096 (2021).

29. Leger, M. et al. Object recognition test in mice. *Nat. Protoc.* **8**, 2531–2537 (2013).

30. Nirogi, R. et al. A simple and rapid method to collect the cerebrospinal fluid of rats and its application for the assessment of drug penetration into the central nervous system. *J. Neurosci. Methods* **178**, 116–119 (2009).

31. Ho, J., Tumkaya, T., Aryal, S., Choi, H. & Claridge-Chang, A. Moving beyond *P* values: Data analysis with estimation graphics. *Nat. Methods* **16**, 565–566. https://doi.org/10.1038/s41592-019-0470-3 (2019).

32. Eddleston, M., Szinicz, L., Eyer, P. & Buckley, N. Oximes in acute organophosphorus pesticide poisoning: A systematic review of clinical trials. *QJM* **95**, 275–283 (2002).

33. Reddy, S. D. & Reddy, D. S. Midazolam as an anticonvulsant antidote for organophosphate intoxication—A pharmacotherapeutic appraisal. *Epilepsia* **56**, 813–821 (2015).

34. Eddleston, M. et al. Speed of initial atropinisation in significant organophosphorus pesticide poisoning—A systematic comparison of recommended regimens. *J. Toxicol. Clin. Toxicol.* **42**, 865–875. https://doi.org/10.1081/CLT-200035223 (2004).

35. Hillman, J., Lehtimäki, K., Peltola, J. & Liimatainen, S. Clinical significance of treatment delay in status epilepticus. *Int. J. Emerg. Med.* **6**, 1–7 (2013).

36. Sharma, S. et al. Role of the Fyn-PKCδ signaling in SE-induced neuroinflammation and epileptogenesis in experimental models of temporal lobe epilepsy. *Neurobiol. Dis.* **110**, 102–121 (2018).

37. Sumadewi, K. T., Harkitasari, S. & Tjandra, D. C. Biomolecular mechanisms of epileptic seizures and epilepsy: A review. *Acta Epileptol.* **5**, 28 (2023).

38. Puttachary, S., Sharma, S., Stark, S. & Thippeswamy, T. Seizure-induced oxidative stress in temporal lobe epilepsy. *BioMed Res. Int.* **2015**, 745613 (2015).

39. Shan, C., Zhang, C. & Zhang, C. The role of IL-6 in neurodegenerative disorders. *Neurochem. Res.* **49**, 834–846 (2024).

40. Putra, M. et al. Inhibiting inducible nitric oxide synthase with 1400W Reduces soman (GD)-induced ferroptosis in long-term epilepsy-associated neuropathology: Structural and functional magnetic resonance imaging correlations with neurobehavior and brain pathology. *J. Pharmacol. Exp. Ther.* **388**, 724–738 (2024).

41. Mirbabaei, F., Mohammad-Khah, A., Babri, M. & Naseri, M. Verification of exposure to sarin nerve agent through the chemical analysis of red blood cell samples. *Microchem. J.* **158**, 105174. https://doi.org/10.1016/j.microc.2020.105174 (2020).

42. Jun, D., Bajgar, J., Kuča, K. & Kassa, J. *Handbook of Toxicology of Chemical Warfare Agents* 1035–1045 (Elsevier, 2020).

43. Zhang, W., Guo, Z., Chen, Y. & Cao, Y. Nanomaterial based biosensors for detection of biomarkers of exposure to op pesticides and nerve agents: A review. *Electroanalysis* **29**, 1206–1213 (2017).

44. Kranawetvogl, T. et al. Evidence of nerve agent VX exposure in rat plasma by detection of albumin-adducts in vitro and in vivo. *Arch. Toxicol.* **97**, 1873–1885. https://doi.org/10.1007/s00204-023-03521-4 (2023).

45. Moyer, R. A., Sidell, F. R. & Salem, H. *Soman* (2014).

46. Agoston, D. V. How to translate time? The temporal aspect of human and rodent biology. *Front. Neurol.* **8**, 92 (2017).

47. McNab, B. K. On the utility of uniformity in the definition of basal rate of metabolism. *Physiol. Zool.* **70**, 718–720 (1997).

48. Massey, N. et al. 1400 W, a selective inducible nitric oxide synthase inhibitor, mitigates early neuroinflammation and nitrooxidative stress in diisopropylfluorophosphate-induced short-term neurotoxicity rat model. *Front. Mol. Neurosci.* **16**, 1125934. https://doi.org/10.3389/fnmol.2023.1125934 (2023).

49. Vezzani, A., Ravizza, T., Balosso, S. & Aronica, E. Glia as a source of cytokines: implications for neuronal excitability and survival. *Epilepsia* **49**, 24–32 (2008).

50. Zhang, Z., Jiang, B. & Gao, Y. Chemokines in neuron-glial cell interaction and pathogenesis of neuropathic pain. *Cell. Mol. Life Sci.* **74**, 3275–3291. https://doi.org/10.1007/s00018-017-2513-1 (2017).

51. Stöberl, N., Maguire, E., Salis, E., Shaw, B. & Hall-Roberts, H. Human iPSC-derived glia models for the study of neuroinflammation. *J. Neuroinflamm.* **20**, 231. https://doi.org/10.1186/s12974-023-02919-2 (2023).

52. Trudler, D. et al. Soluble α-synuclein-antibody complexes activate the NLRP3 inflammasome in hiPSC-derived microglia. *Proc. Natl. Acad. Sci. U.S.A.* **118**, e2025847118. https://doi.org/10.1073/pnas.2025847118 (2021).

53. Badanjak, K. et al. iPSC-derived microglia as a model to study inflammation in idiopathic Parkinson's disease. *Front. Cell Dev. Biol.* **9**, 740758. https://doi.org/10.3389/fcell.2021.740758 (2021).

54. Tapia-Abellán, A. et al. Sensing low intracellular potassium by NLRP3 results in a stable open structure that promotes inflammasome activation. *Sci. Adv.* **7**, eabf4468. https://doi.org/10.1126/sciadv.abf4468 (2021).

55. Minkiewicz, J., Vaccari, J. & Keane, R. Human astrocytes express a novel NLRP2 inflammasome. *Glia* **61**, 1113–1121. https://doi.org/10.1002/glia.22499 (2013).

56. Li, W., Xiao, H., Wu, H., Xu, X. & Zhang, Y. Organophosphate pesticide exposure and biomarkers of liver injury/liver function. *Liver Int.* **42**, 2713–2723. https://doi.org/10.1111/liv.15461 (2022).

57. Alvarez-Alvarez, I. & Andrade, R. J. Organophosphate pesticides: Another silent liver hazard?. *Liver Int.* **43**, 268–170 (2023).

58. Rubio, C. R., FelipeFernández, C., Manzanedo Bueno, R., Del Pozo, B. A. & García, J. M. Acute renal failure due to the inhalation of organophosphates: Successful treatment with haemodialysis. *Nephrol. Dial. Transplant. Plus* **5**, 582–583 (2012).

59. Tsai, K.-F., Lee, W.-C., Lee, C.-T. & Kung, C.-T. # 6546 renal tubular toxicity of organophosphate flame retardants in patients with chronic kidney disease. *Nephrol. Dial. Transplant.* **38**, i1158–i1159 (2023).

60. Ferguson, M. & Waikar, S. Established and emerging markers of kidney function. *Clin. Chem.* **58**, 680–689. https://doi.org/10.1373/clinchem.2011.167494 (2012).

61. Gounden, V., Bhatt, H. & Jialal, I. *Renal Function Tests* (StatPearls Publishing, 2023).

62. Molitoris, B. A. Low-flow acute kidney injury: The pathophysiology of prerenal azotemia, abdominal compartment syndrome, and obstructive uropathy. *Clin. J. Am. Soc. Nephrol.* **17**, 1039–1049 (2022).

63. Serafini, M. A., Paz, A. H. & Nunes, N. S. Cholinergic immunomodulation in inflammatory bowel diseases. *Brain Behav. Immun. Health* **19**, 100401 (2022).

64. Gage, M., Vinithakumari, A. A., Mooyottu, S. & Thippeswamy, T. Gut dysbiosis following organophosphate, diisopropylfluorophosphate (DFP), intoxication and saracatinib oral administration. *Front. Microb.* **1**, 1006078 (2022).

65. Clewell Iii, H. J. & Andersen, M. E. Dose, species, and route extrapolation using physiologically based pharmacokinetic models. *Drink. Water Health Pharmacokinet. Risk Assess.* **8**, 159 (1987).

Author contributions

NM and SSV conducted experiments and analyzed the data. NM and TT contributed significantly to manuscript writing. NM and SSV performed data analysis and cross verified by TT. LGGL provided equipment for multiplex analysis. TH analyzed Liver and Kidney tissue and performed Histopathological scoring evaluation. TT conceptualized the project, wrote the grant, supervised the work, acquired funding and managed the project.

Declarations

Competing interests

The authors declare no competing interests.

Ethics approval and consent to participate

The experiments were conducted per the approved protocols by the Institutional Animal Care and Use Committees (IACUC protocol: 23–114) and complied with the NIH ARRIVE Guidelines for the Care and Use of Laboratory Animals.

Consent for publication

All authors agreed to publish.

Additional information

Supplementary Information The online version contains supplementary material available at https://doi.org/10.1038/s41598-025-94190-z.

Correspondence and requests for materials should be addressed to T.T.

Reprints and permissions information is available at www.nature.com/reprints.

Publisher's note Springer Nature remains neutral with regard to jurisdictional claims in published maps and institutional affiliations.